MASS LOADING OF BOW-SHOCK PULSAR WIND NEBULAE

Giovanni Morlino

INFN/GSSI, L'Aquila, Italy
Purdue University, INDIANA

In collaboration with:
M. Lyutikov & M. Vorster

Accepted for publication in MNRAS (arXiv:1505.01712)

High Energy Phenomena in Relativistic Outflow V
La Plata, 5-8 October 2015


SN 1006
NASA/ESA/Hubble Heritage Team
(STScI/AURA)

THE BASIC PICTURE

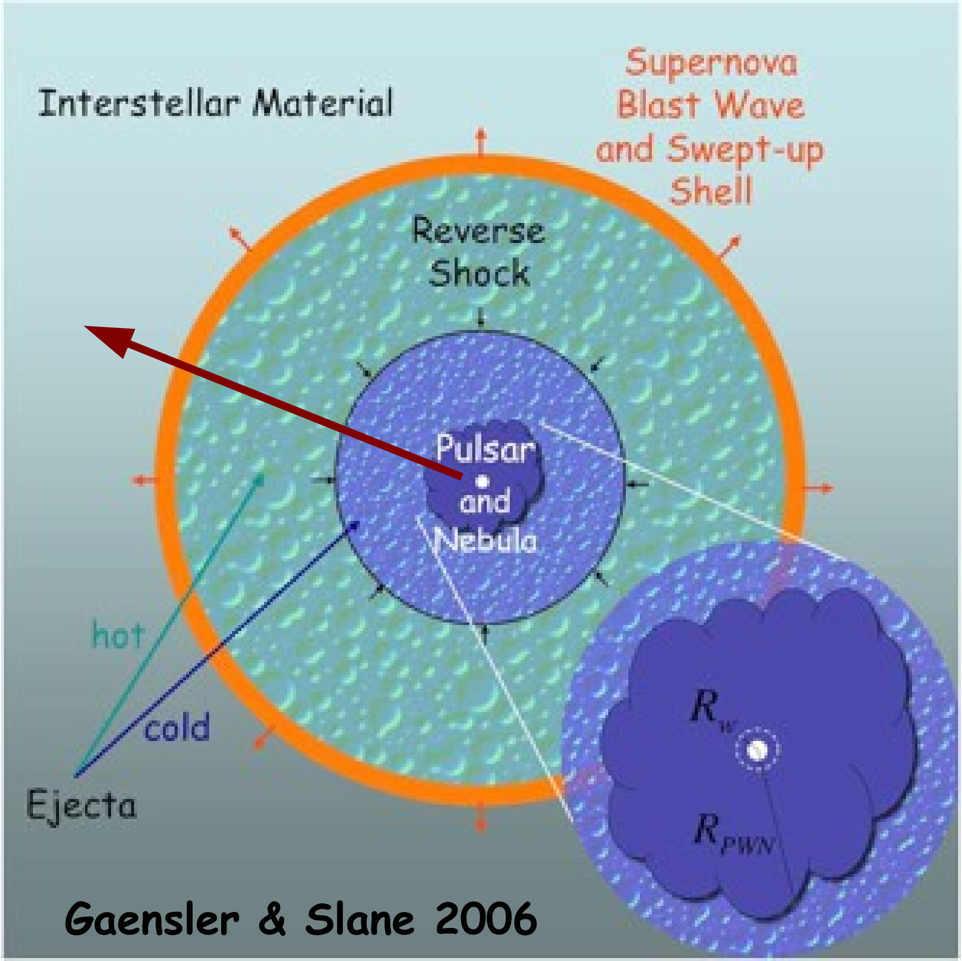

Gaensler & Slane 2006

If the kick velocity of the NS >~ 100 km/s

⇩

Pulsar can escape from the SNR when it is enough powerful to be observed

Structure of bow-shock nebula

Typical NS speed: V_{NS} ~ 100-500 km/s → Mach number >10 (highly supersonic)

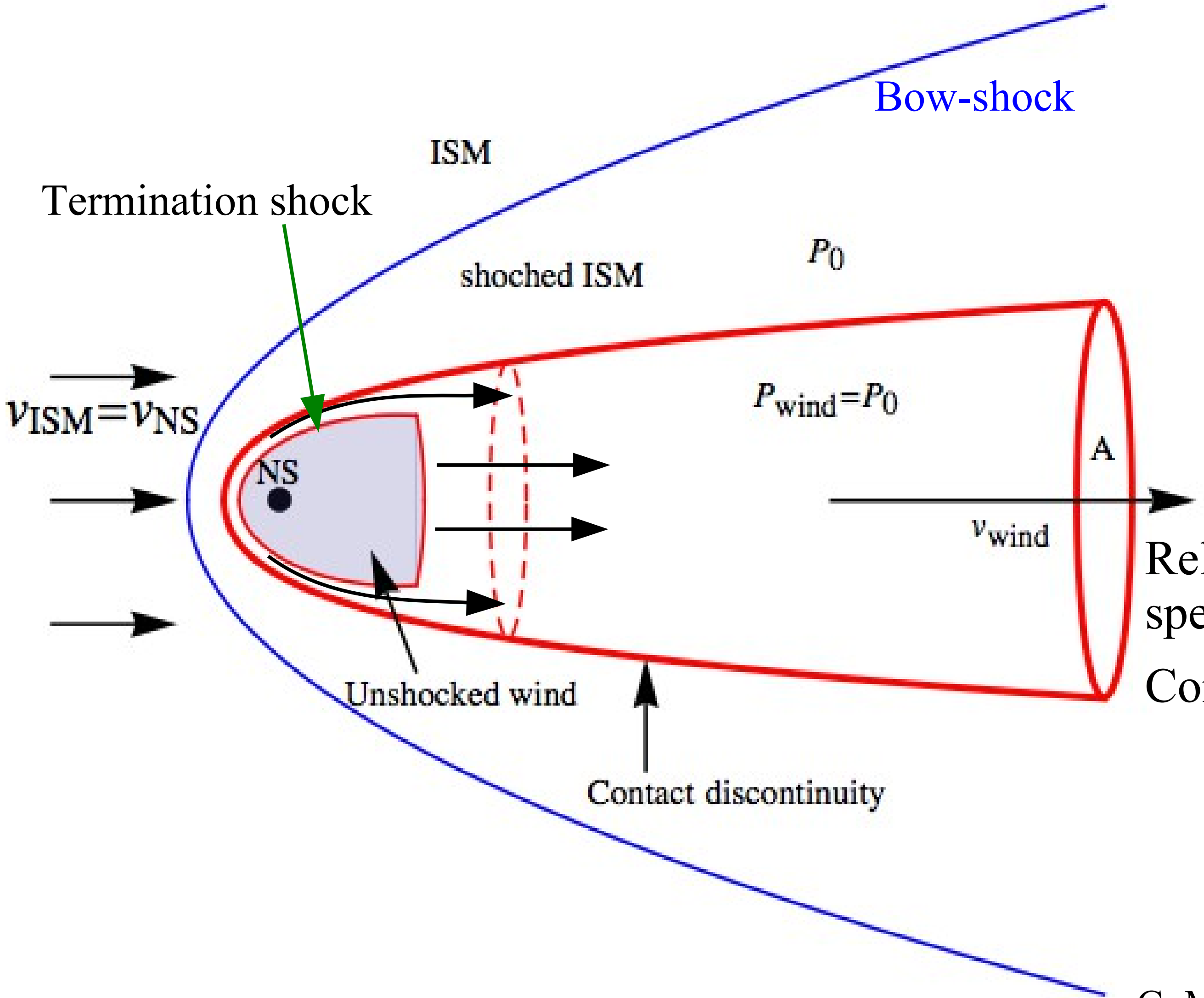

Relativistic wind
speed: V_{wind} ~ 0.1-0.9 c
Composition: mainly pairs $e^{\pm}$

Structure of bow-shock nebula from simulations

[From Bucciantini, Amato & del Zanna 2005, *A&A* 434,189]

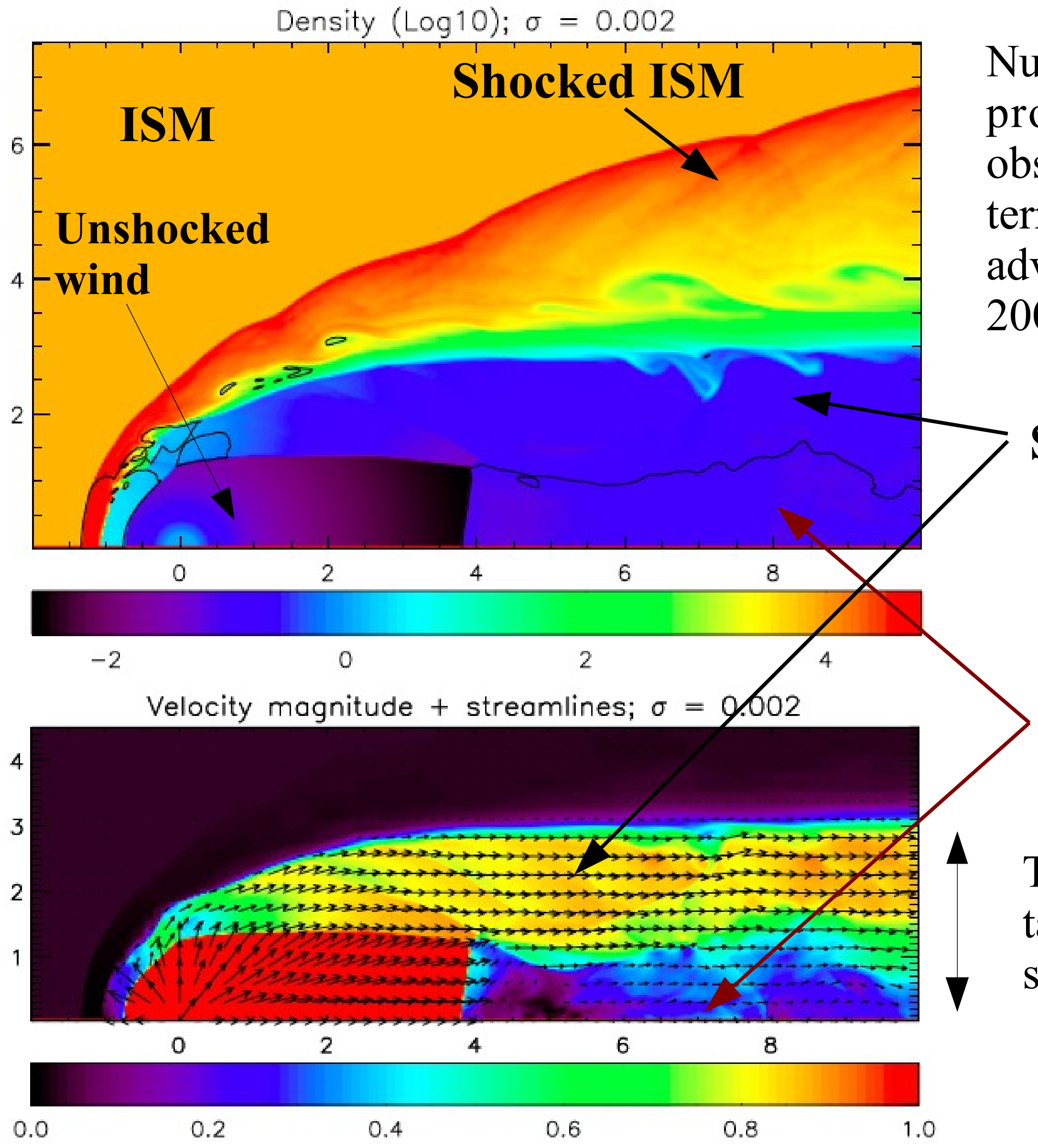

Numerical MHD models (Bucciantini et al. 2005) produce images that could be compared to observations but simulations go out just to a ~10 termination shock radii. Analytical models may offer advantages (e.g., Romanova, Chulsky, & Lovelace 2005).

Supersonic wind

Subsonic wind

NO NEUTRALS

The wind is collimated in a cylindrical tale with constant area within the whole simulation box

Bowshock-tail PWNe in X-rays

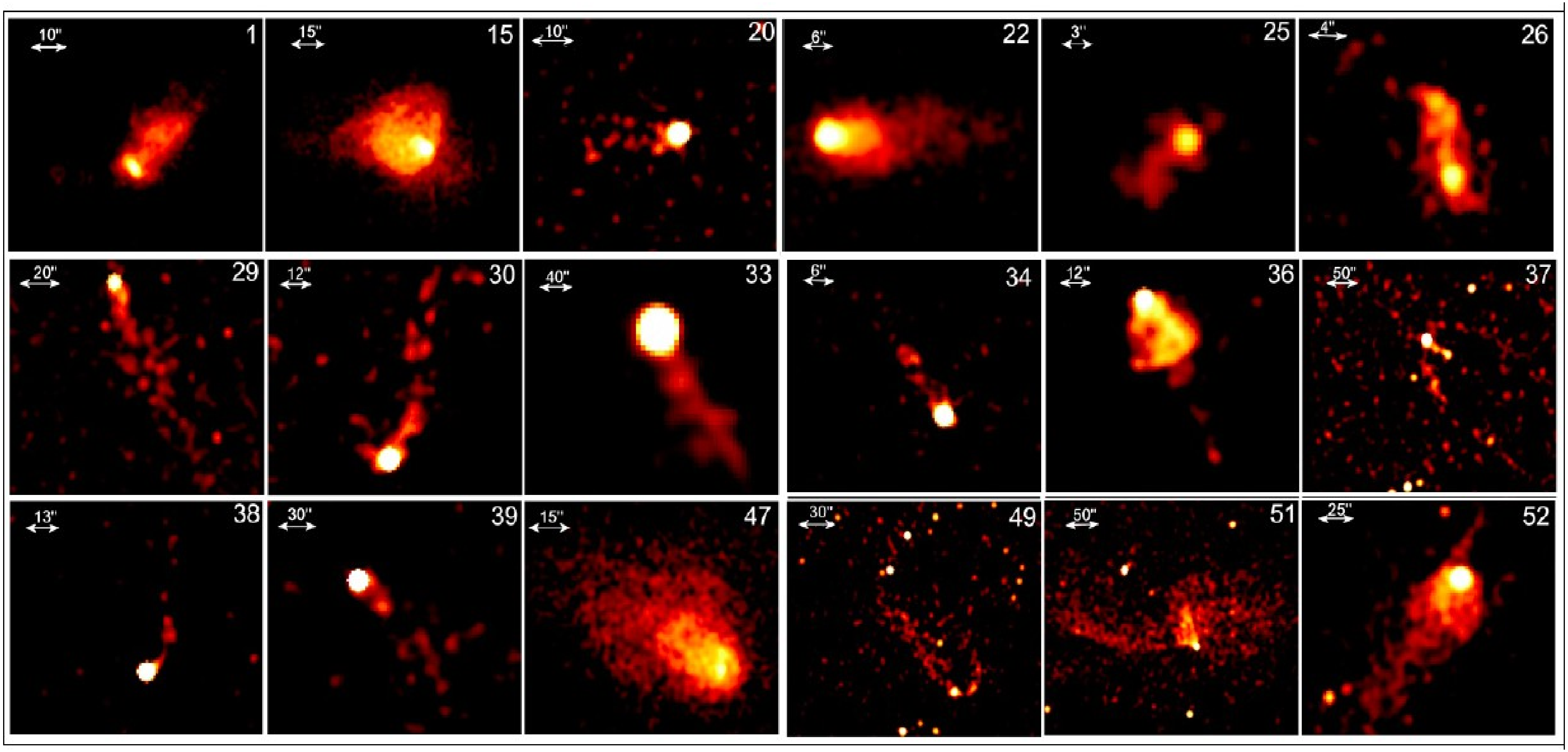

[Pictures from O. Kargaltsev]

Structure of bow-shock nebula in presence of neutrals

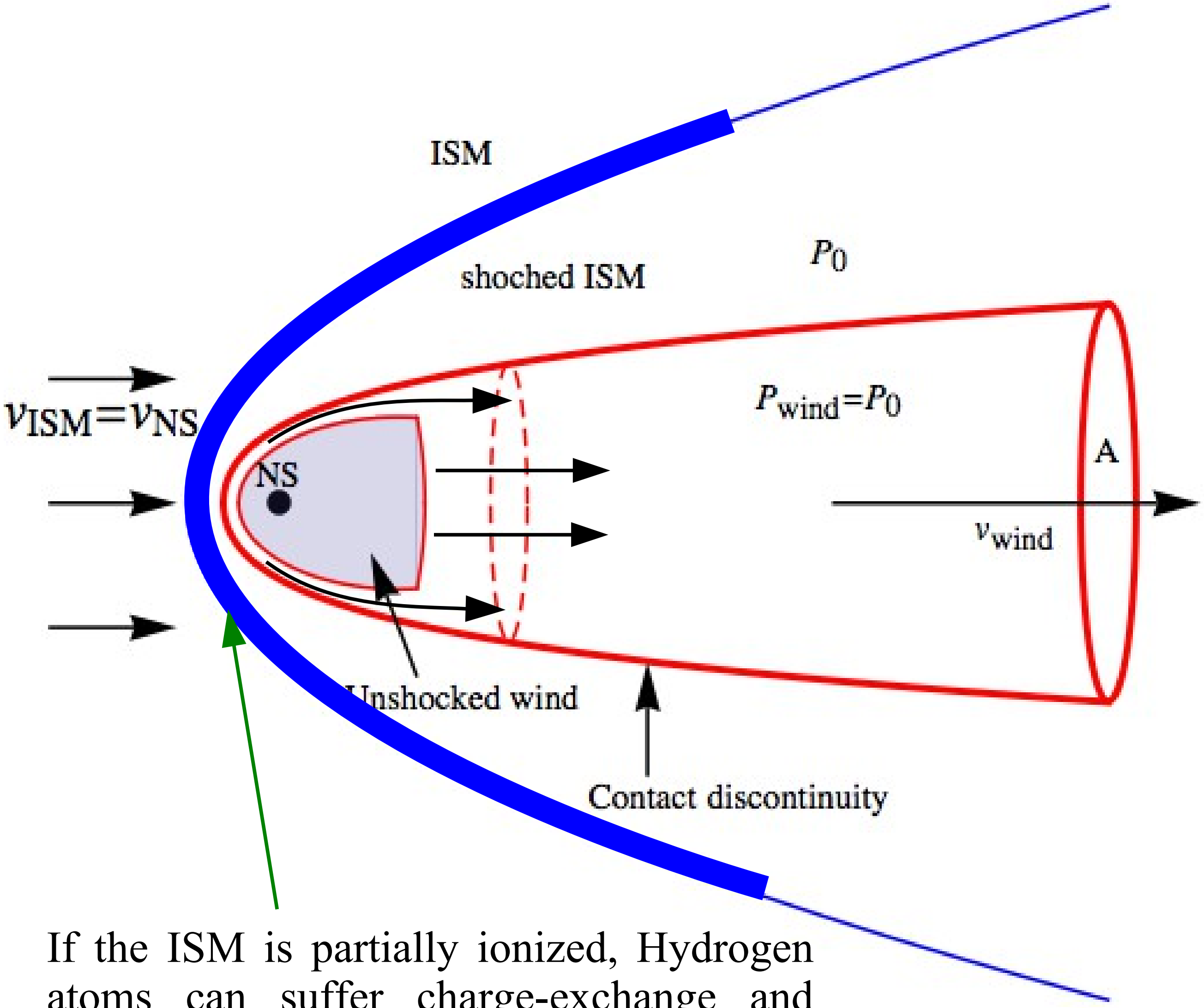

If the ISM is partially ionized, Hydrogen atoms can suffer charge-exchange and collisional excitation emitting Balmer lines

Structure of bow-shock nebula in presence of neutrals

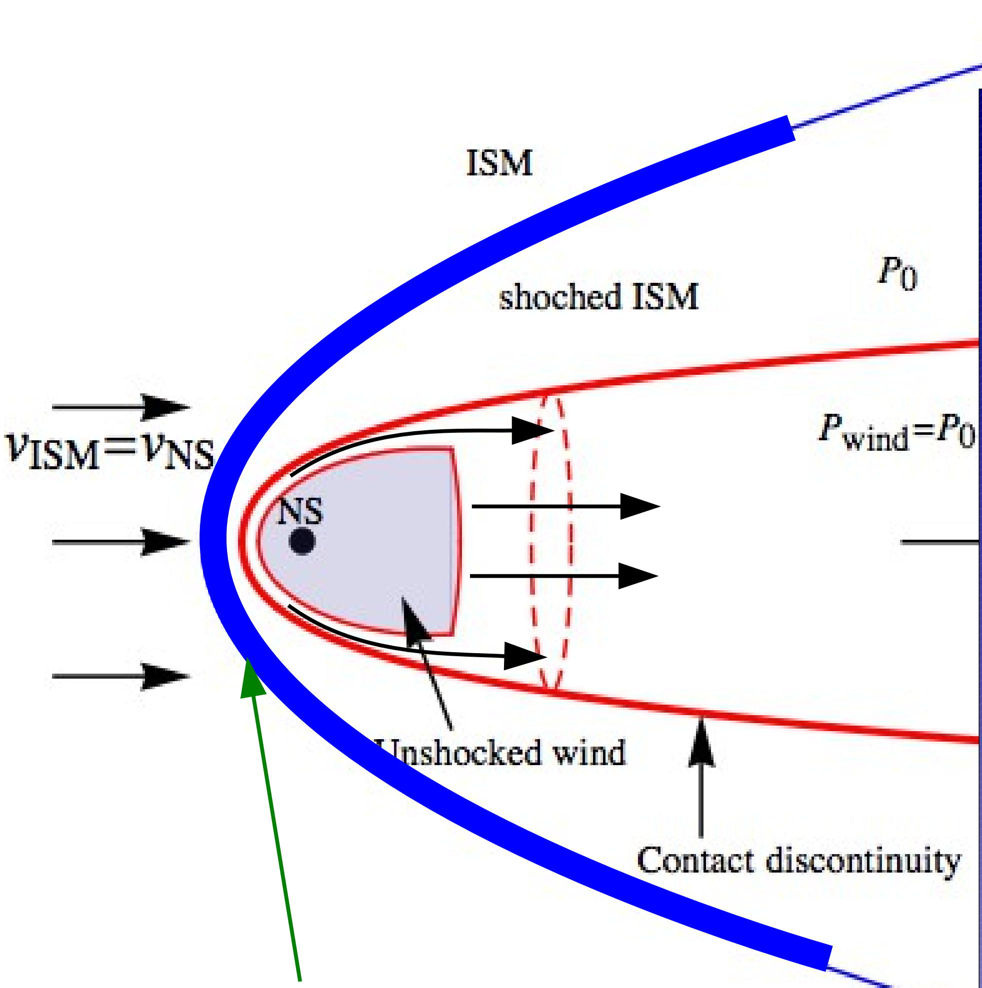

If the ISM is partially ionized, Hydrogen atoms can suffer charge-exchange and collisional excitation emitting Balmer lines

Hα emission from J0437-4714

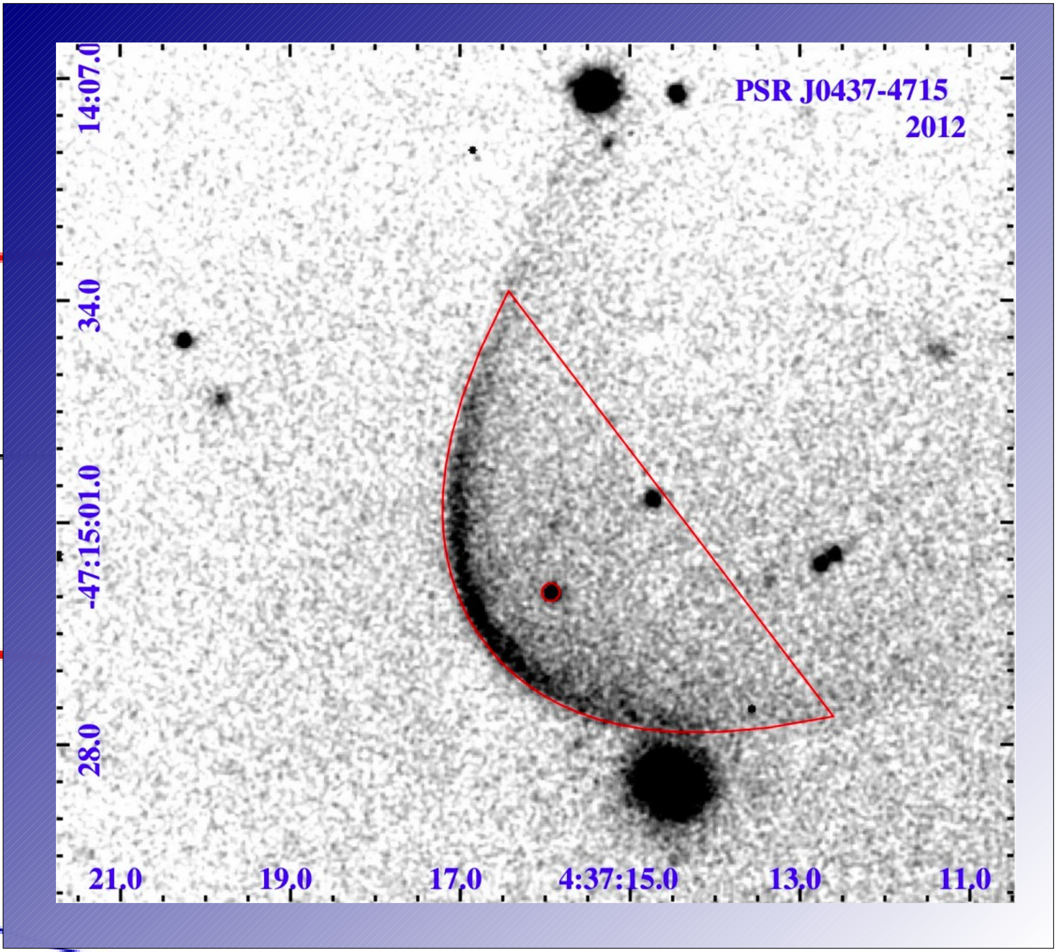

Summary of pulsar with Hα bow shock

[From Brownsberger & Romani 2014, arXiv:1402.5465]

- 6 over 9 known Hα bow shock nebulae show rapid expansion and/or contraction of the tale
- These features are axisymmetric along the propagation axes of the pulsar

This suggest that the tale could be modified by internal dynamics rather than by external effects (non uniform ISM)

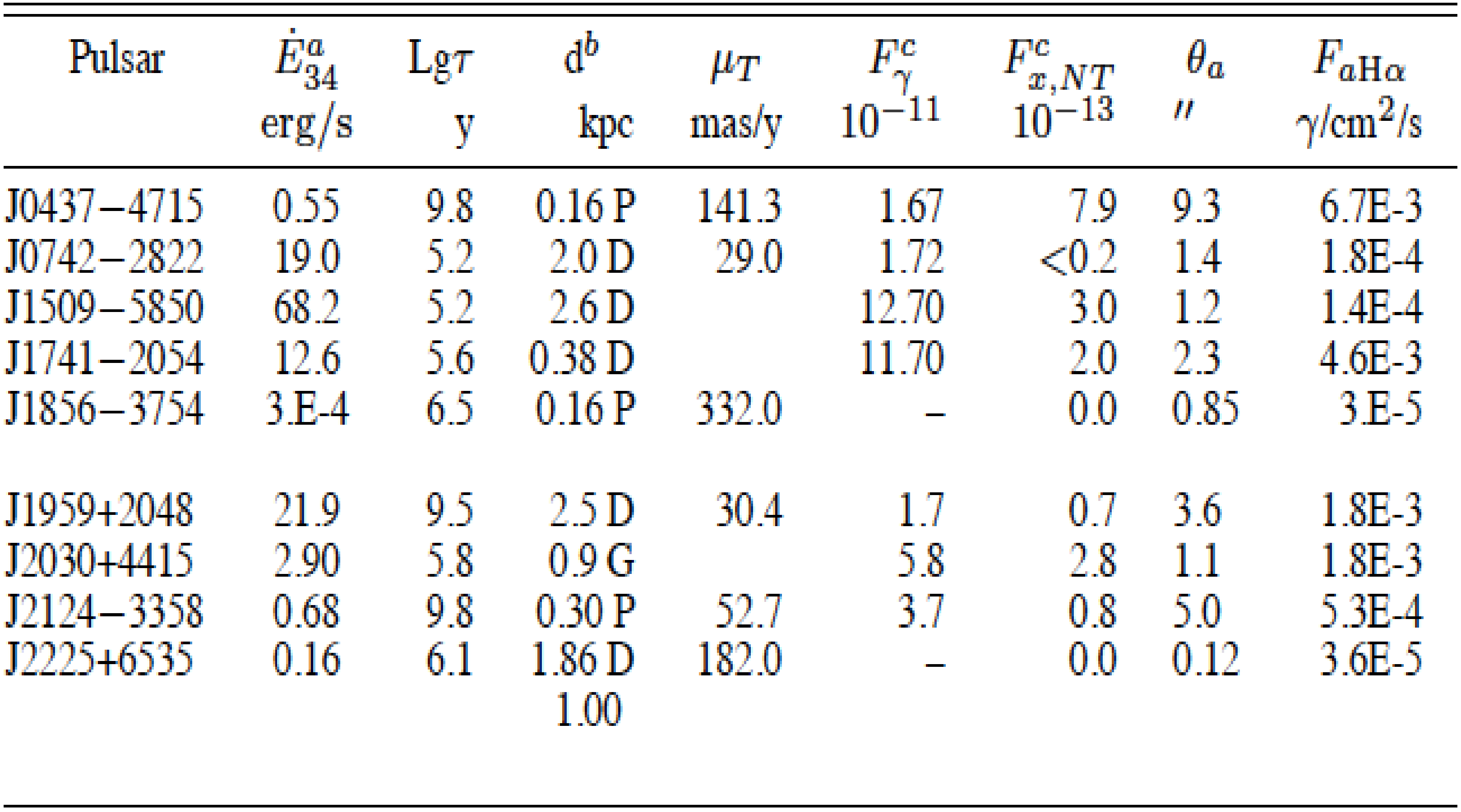

Cometary shape

Anomaluos features

Pulsar	$\dot{E}_{34}^{a}$ erg/s	Lgτ y	d^{b} kpc	μ_T mas/y	F_{γ}^{c} 10^{-11}	$F_{x,NT}^{c}$ 10^{-13}	θ_a ″	$F_{aH\alpha}$ γ/cm^2/s
J0437−4715	0.55	9.8	0.16 P	141.3	1.67	7.9	9.3	6.7E-3
J0742−2822	19.0	5.2	2.0 D	29.0	1.72	<0.2	1.4	1.8E-4
J1509−5850	68.2	5.2	2.6 D		12.70	3.0	1.2	1.4E-4
J1741−2054	12.6	5.6	0.38 D		11.70	2.0	2.3	4.6E-3
J1856−3754	3.E-4	6.5	0.16 P	332.0	–	0.0	0.85	3.E-5
J1959+2048	21.9	9.5	2.5 D	30.4	1.7	0.7	3.6	1.8E-3
J2030+4415	2.90	5.8	0.9 G		5.8	2.8	1.1	1.8E-3
J2124−3358	0.68	9.8	0.30 P	52.7	3.7	0.8	5.0	5.3E-4
J2225+6535	0.16	6.1	1.86 D 1.00	182.0	–	0.0	0.12	3.6E-5

Guitar nebula (powered by PRS B2224+65)

[From Gautam A. et al. 2013]

Balmer emission:
images from HST

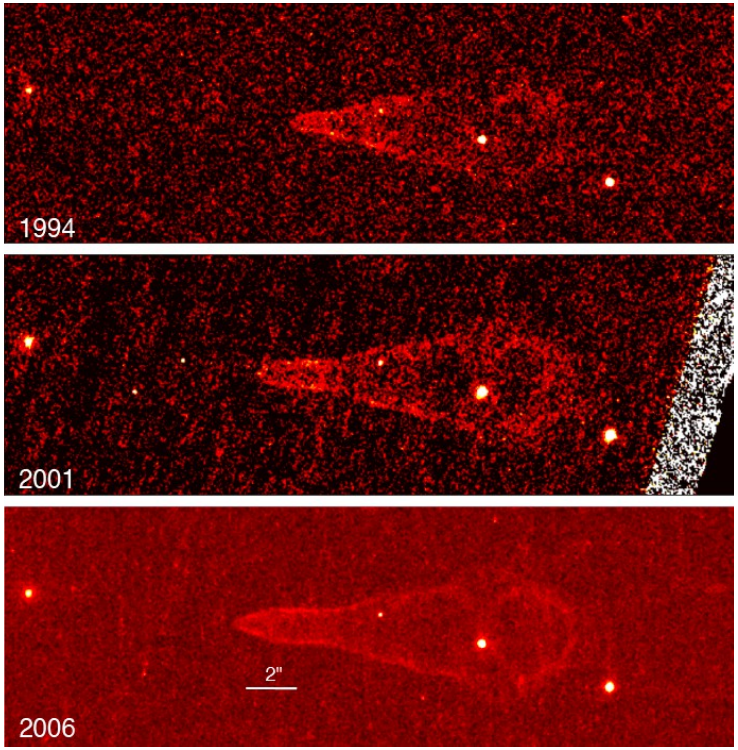

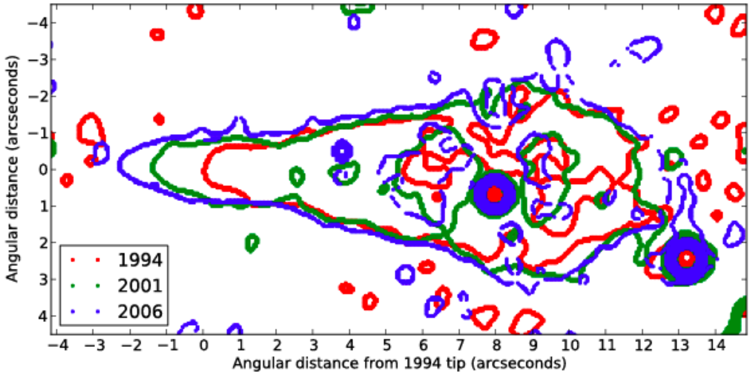

From Palomar Observatory (1995)

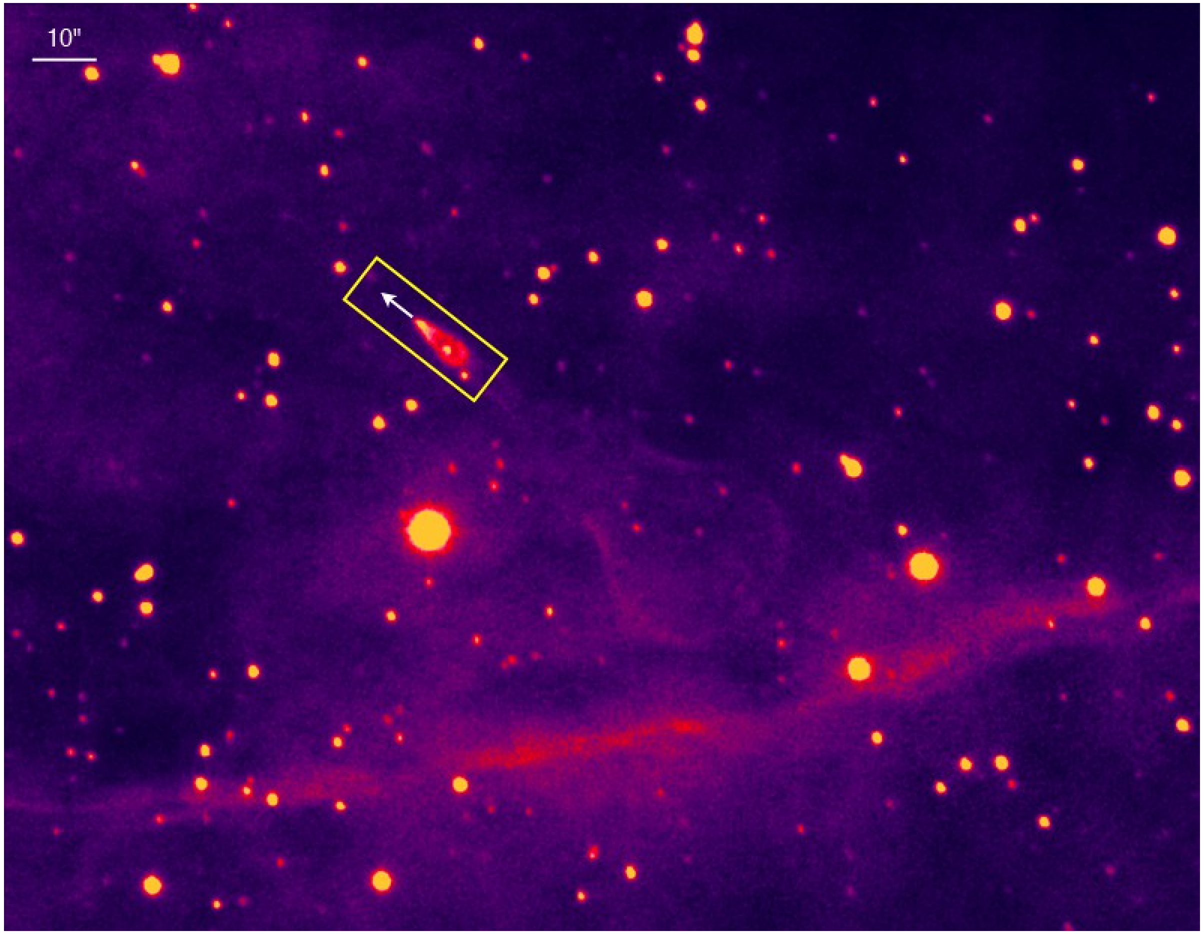

PSR J2124-3358

[From Brownsberger & Romani 2014, *ApJ* accepted arXiv:1402.5465]

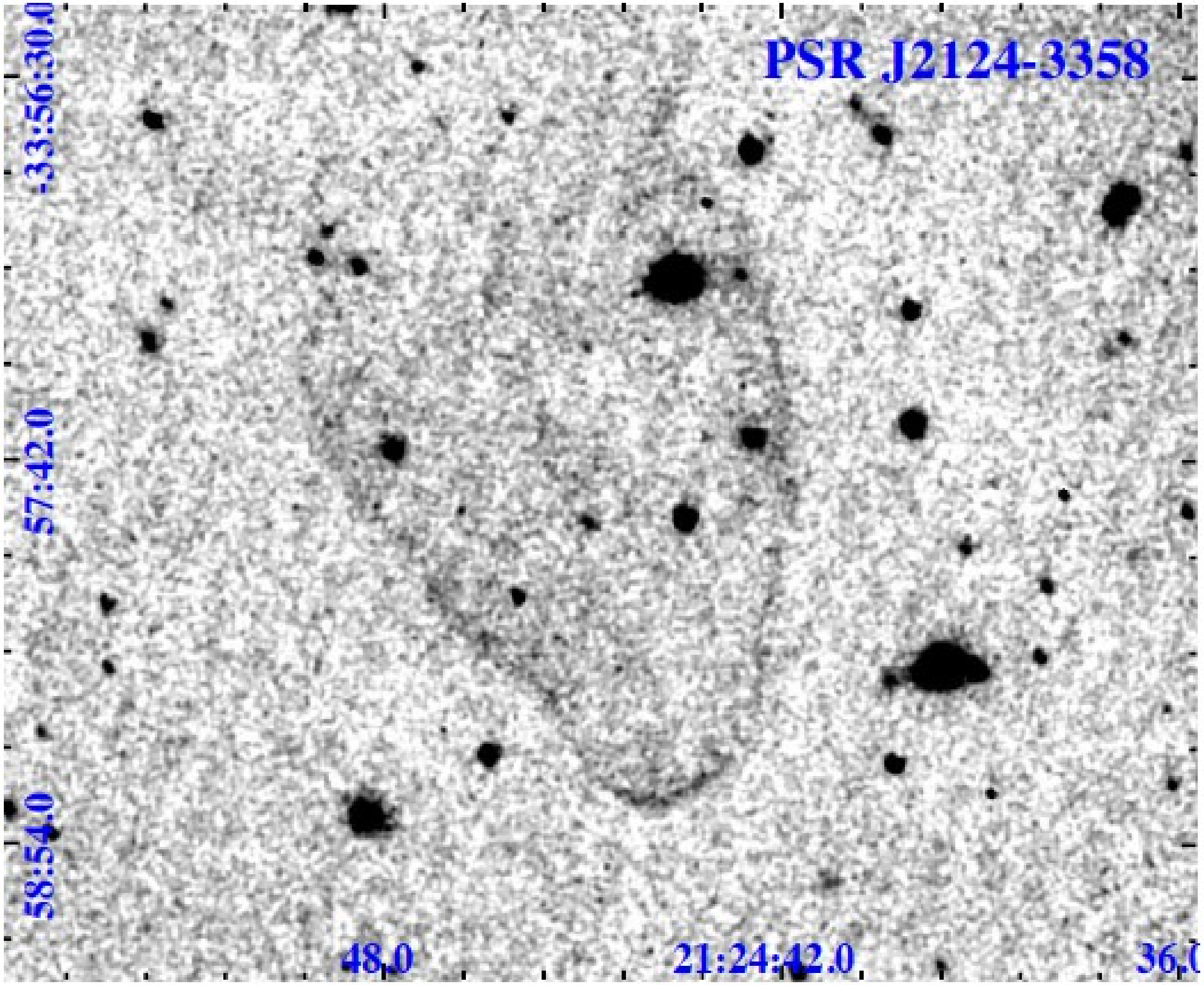

PSR J2124-3358

[From Brownsberger & Romani 2014, *ApJ* accepted arXiv:1402.5465]

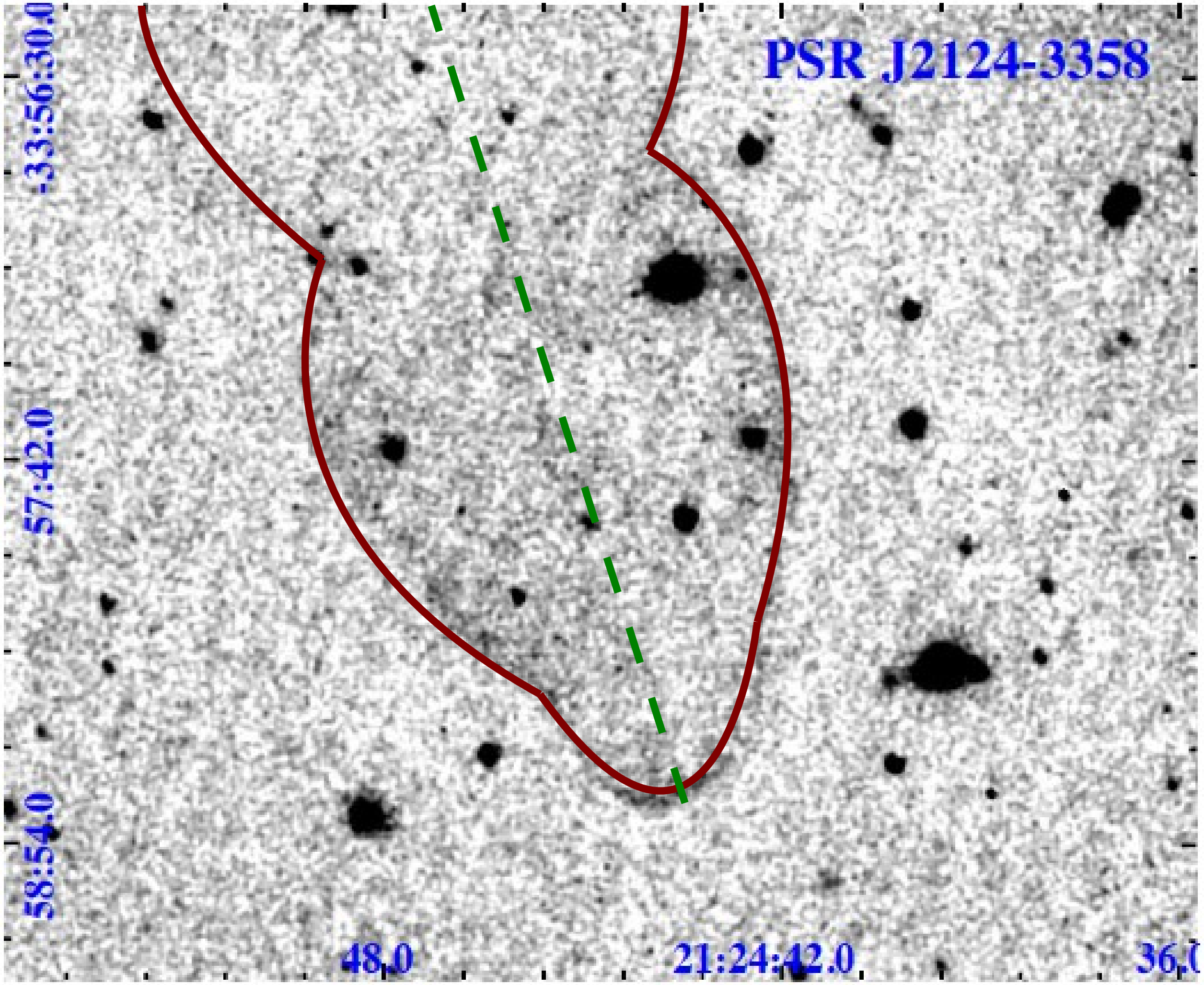

PSR J2124-3358

[From Brownsberger & Romani 2014, *ApJ* accepted arXiv:1402.5465]

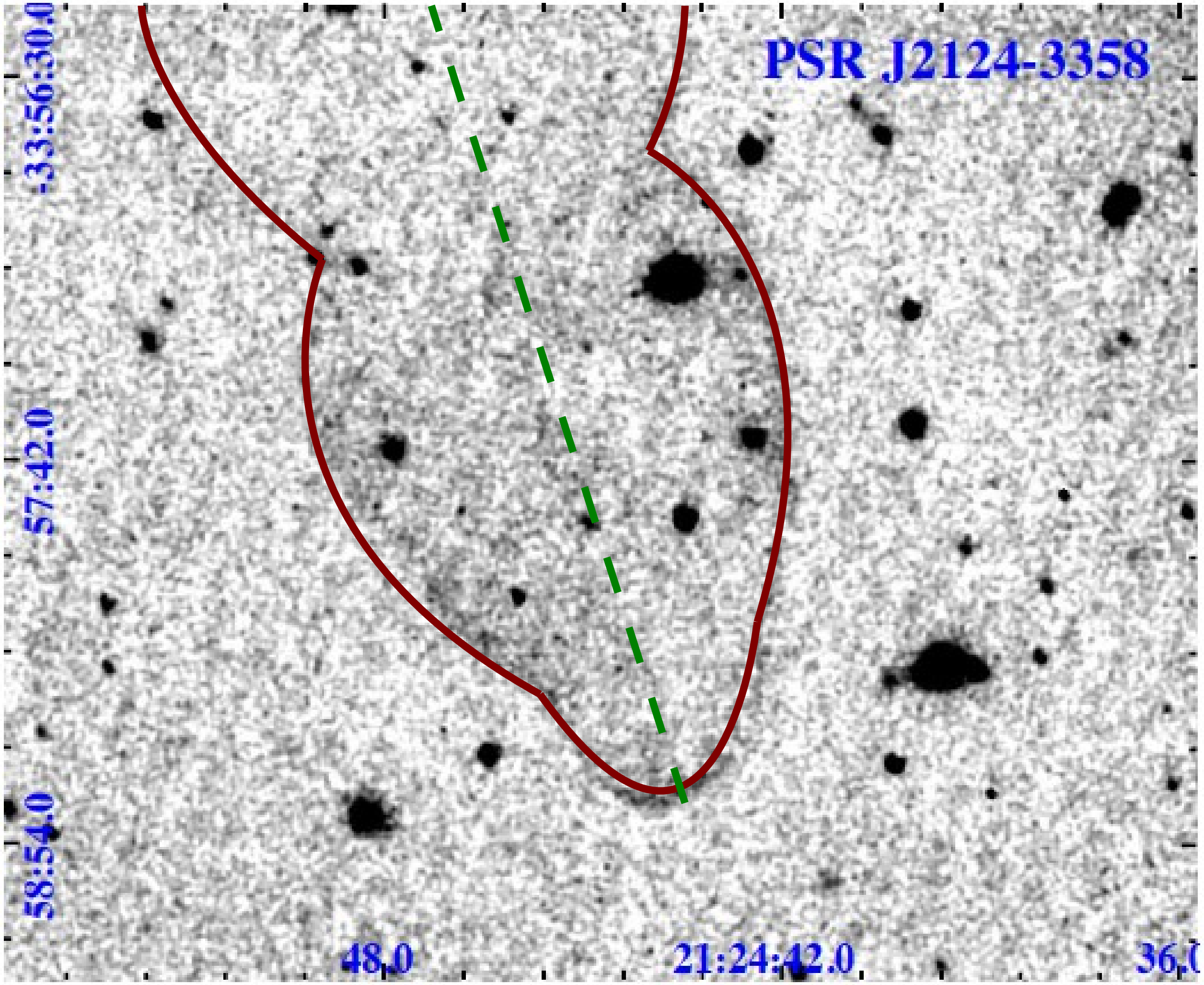

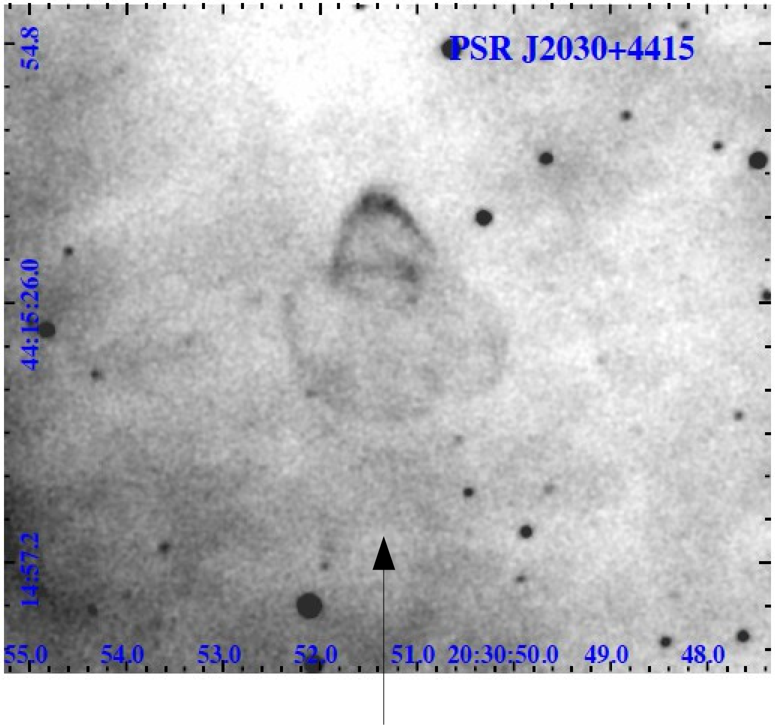

New discovered with a survey for Hα bow shock emission around nearby FermiLAT γ-detected energetic pulsars

PSR J0742-2822

[From Brownsberger & Romani 2014, *ApJ*, arXiv:1402.5465]

Hα image with background star light subtracted

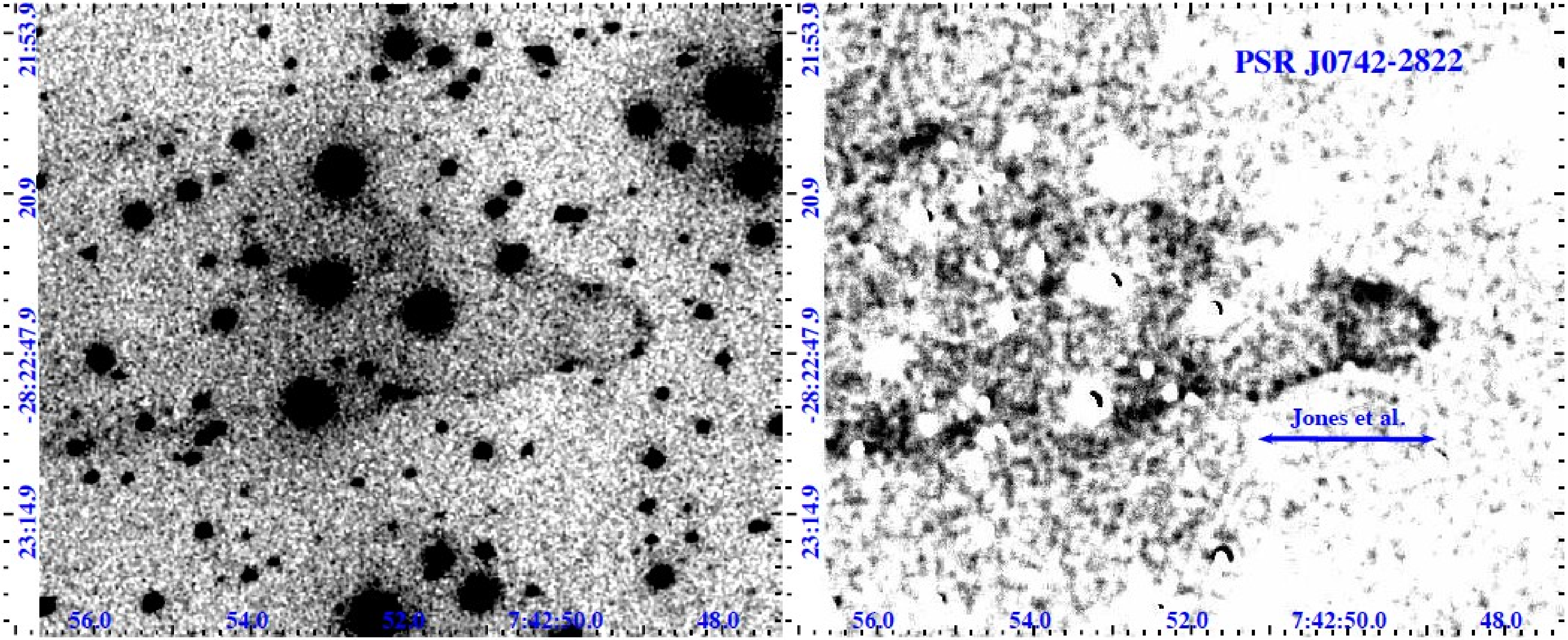

Interaction length-scales for neutrals

$$d_S=\left(\frac{L_{wind}}{4\pi V_{NS}^2\rho_0 c}\right)^{1/2} = 4\cdot 10^{15}\left(\frac{L_{wind}}{10^{34}\,erg}\right)^{1/2}\left(\frac{V_{NS}}{300\,km/s}\right)\left(\frac{n_0}{cm^{-3}}\right)^{-1/2} cm$$

Stagnation distance

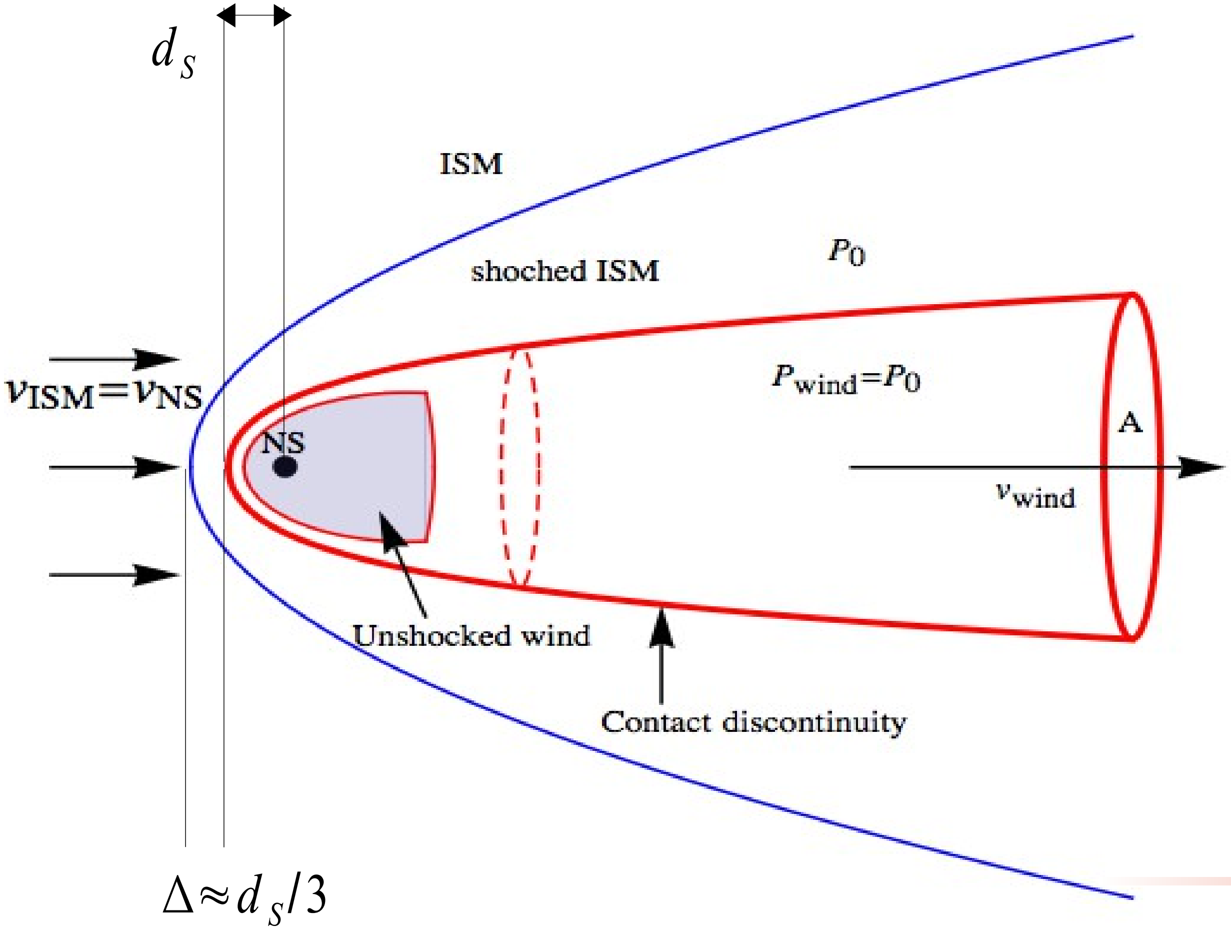

Interaction length-scales for neutrals

$$d_S = \left(\frac{L_{wind}}{4\pi V_{NS}^2 \rho_0 c} \right)^{1/2} = 4\cdot 10^{15} \left(\frac{L_{wind}}{10^{34}\, erg} \right)^{1/2} \left(\frac{V_{NS}}{300\, km/s} \right) \left(\frac{n_0}{cm^{-3}} \right)^{-1/2} cm$$

Stagnation distance

$$\lambda_{coll} = \frac{V_{NS}}{x_{ion}\, n_{ISM} \langle \sigma_{coll}\, v_{rel} \rangle} \rightarrow \begin{cases} \lambda_{CE} = 1.3\cdot 10^{15} \quad cm \quad \sim \quad d_S \\ \lambda_{ion,e} \approx 1.0\cdot 10^{15} \quad cm \quad \sim \quad d_S \\ \lambda_{ion,p} = 3.0\cdot 10^{20} \quad cm \quad \gg d_S \end{cases}$$

Collisional length-scale in the shocked ISM

Neutral Hydrogen from the ISM can penetrate into the wind region (V_{NS} = 300 km/s, ion fraction=10%)

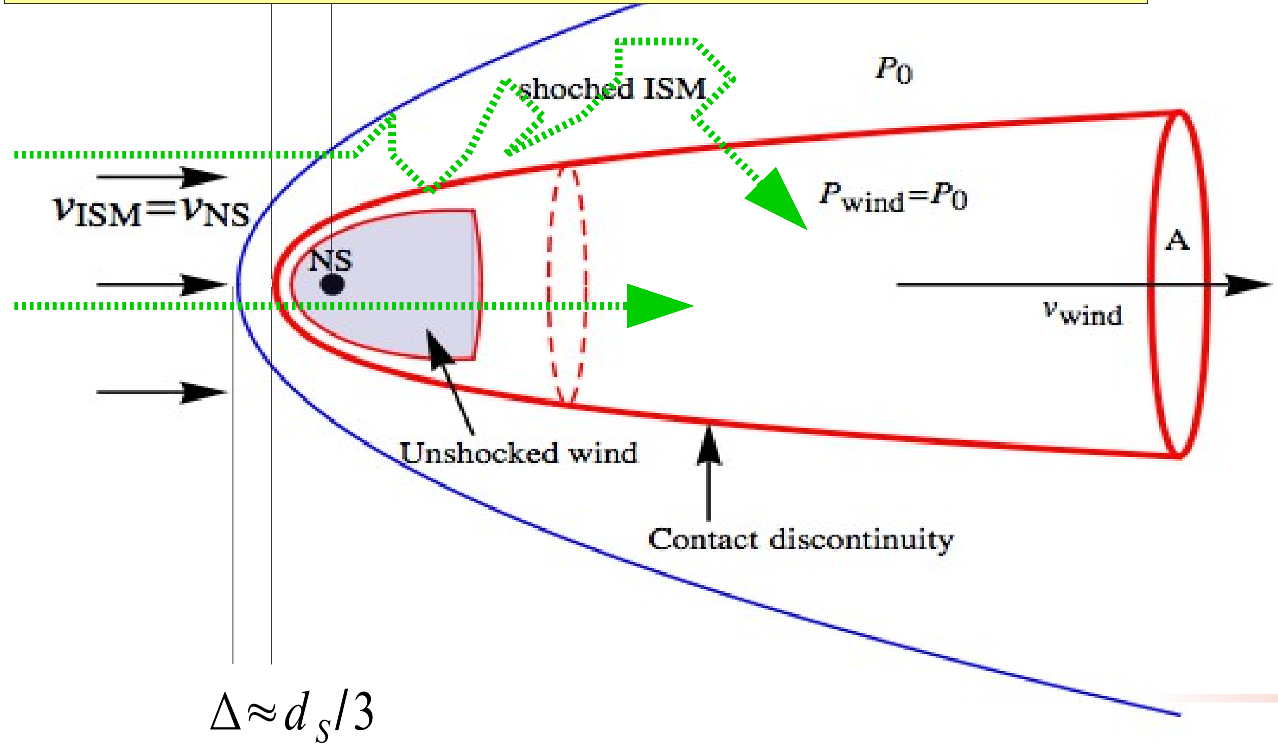

Interaction length-scales for neutrals

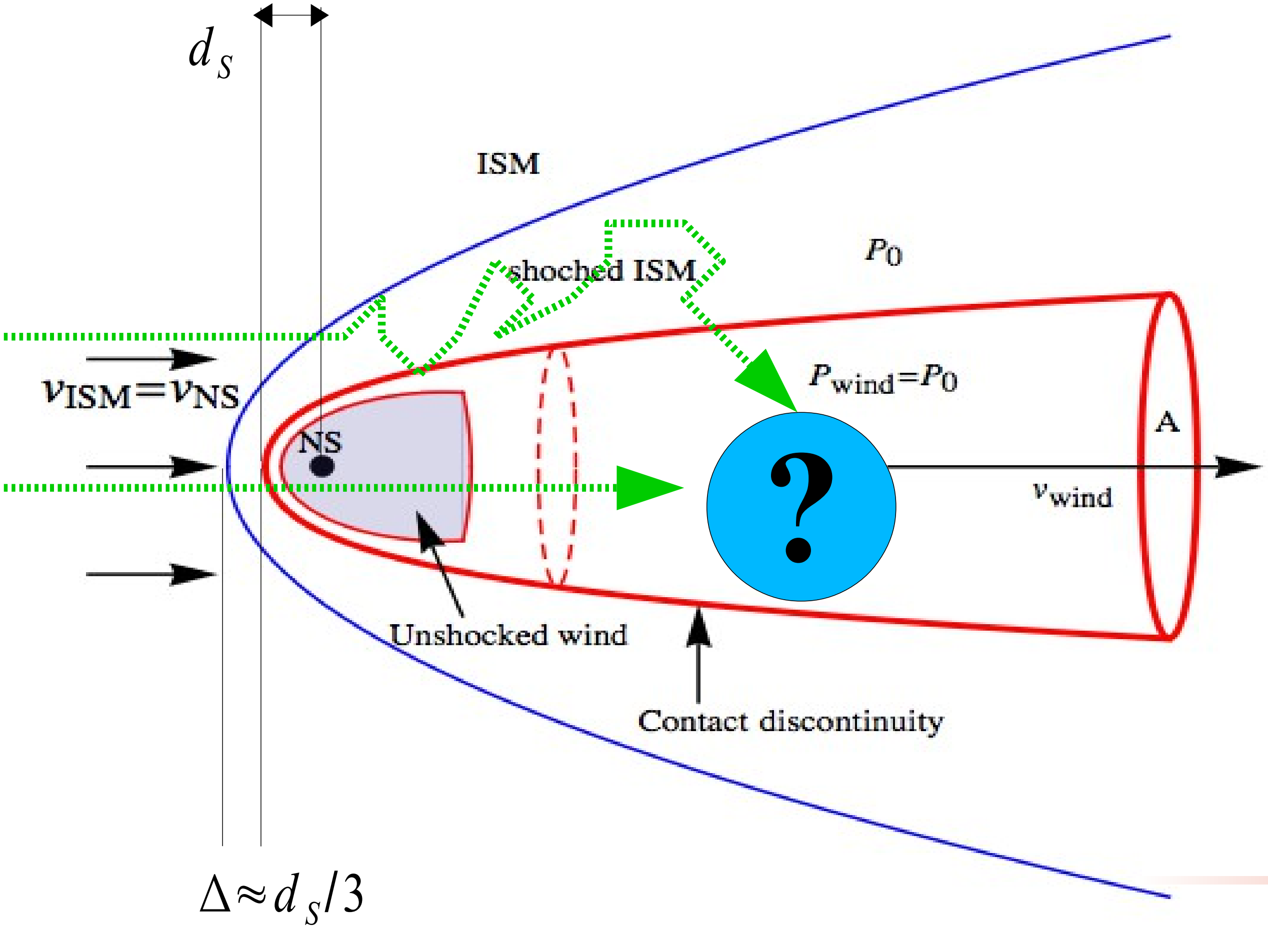

Interaction length-scales for neutrals

$$\lambda_{ion,wind} = \frac{V_{NS}}{n_e \sigma_{Bethe} c} \approx 4\cdot 10^{23}\left(\frac{V_{SN}}{300\,km/s}\right)\left(\frac{n_e}{10^{-10}\,cm^{-3}}\right)^{-1} cm$$

Ionization length scale of hydrogen due to collision with relativistic electrons

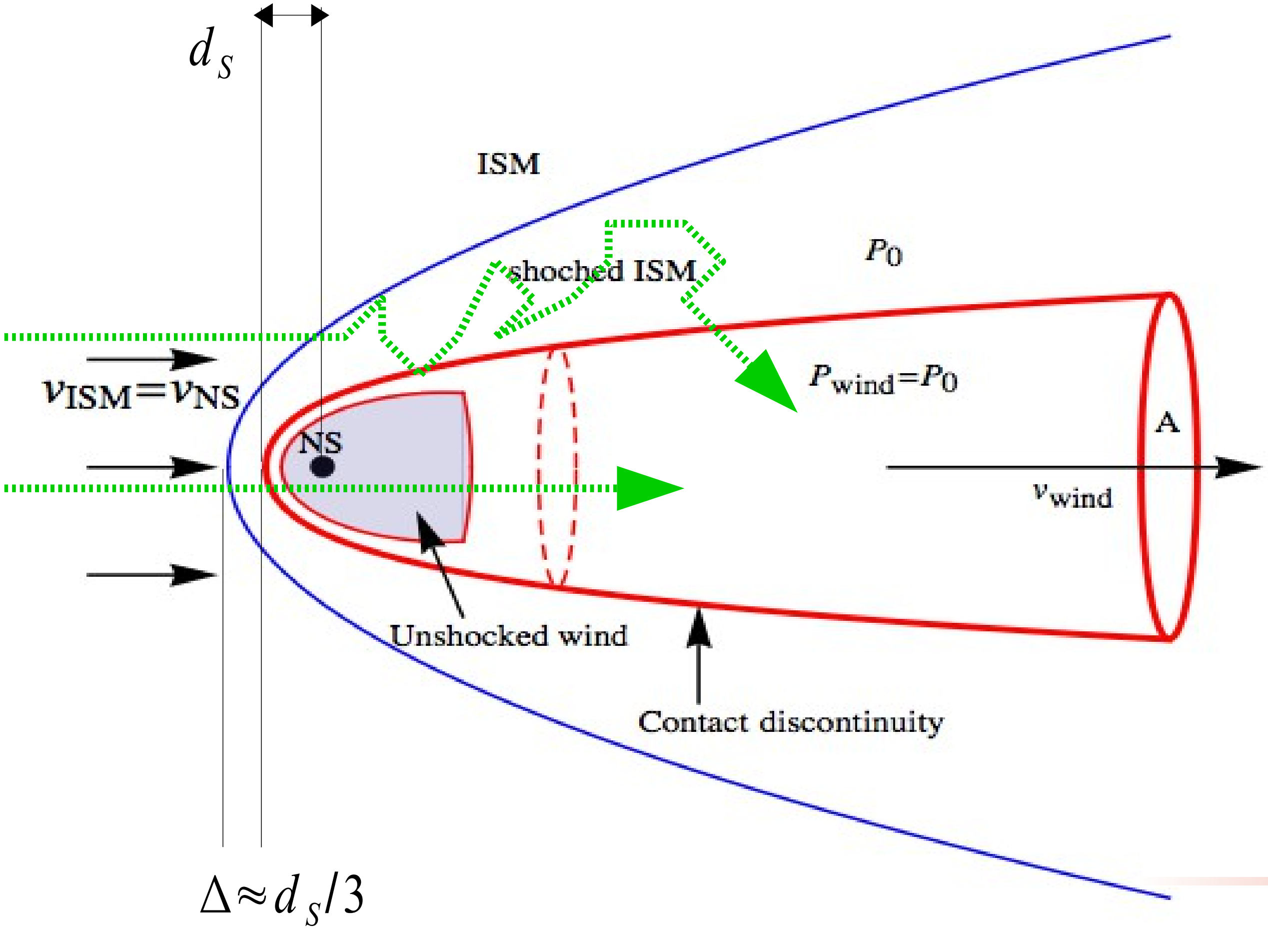

Interaction length-scales for neutrals

$$\lambda_{ion,wind} = \frac{V_{NS}}{n_e \sigma_{Bethe} c} \approx 4\cdot 10^{23} \left(\frac{V_{SN}}{300\,km/s}\right) \left(\frac{n_e}{10^{-10}\,cm^{-3}}\right)^{-1} cm$$

Ionization length scale of hydrogen due to collision with relativistic electrons

Length scale for photo-ionization due to non-thermal UV radiation from the nebula:

$$\lambda_{ph-ion} = \frac{V_{NS}}{n_{ph} \bar{\sigma}_{ph} c} \approx 3\cdot 10^{14} \left(\frac{R}{d_S}\right) \left(\frac{\eta_X}{10^{-4}}\right)^{-1} \left(\frac{V_{NS}}{300\,km/s}\right)^{-1} \left(\frac{n_0}{1\,cm^{-3}}\right)^{-1} F(\Gamma)\ cm \approx 10^{14} - 10^{17}\,cm$$

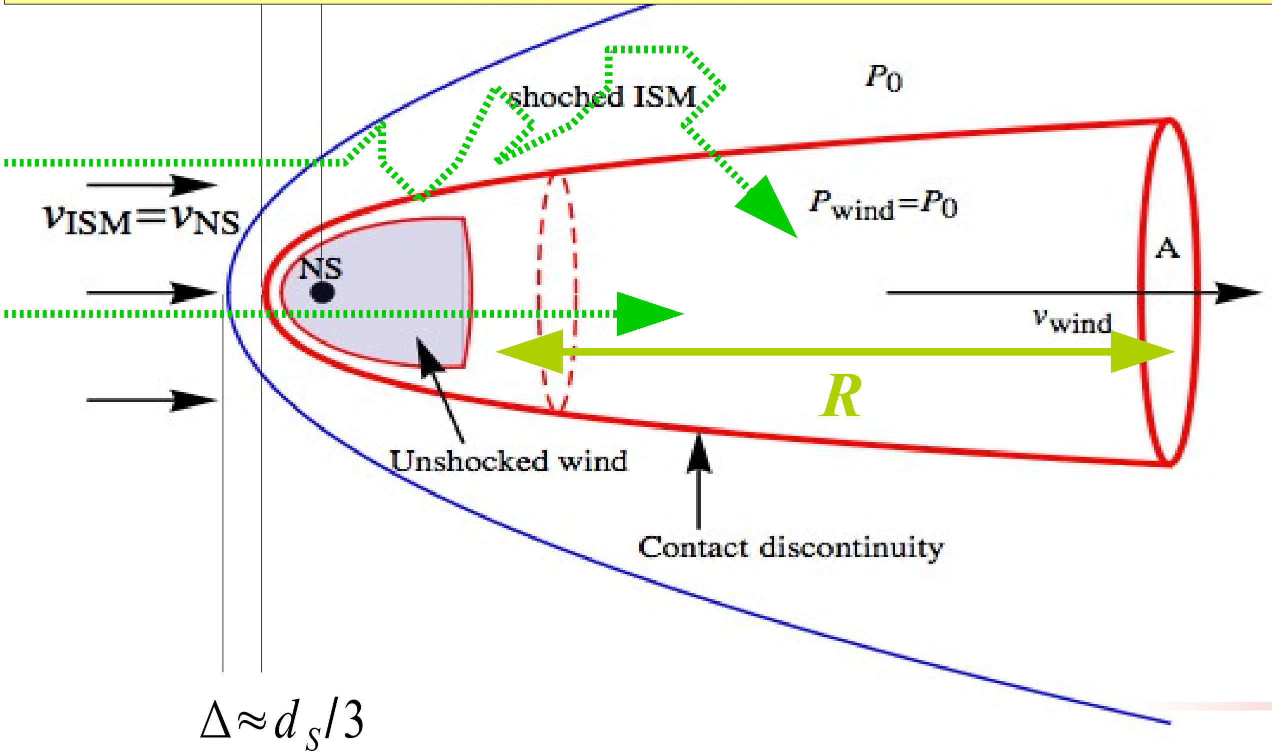

Interaction length-scales for neutrals

$$\lambda_{ion,wind} = \frac{V_{NS}}{n_e \sigma_{Bethe}\, c} \approx 4 \cdot 10^{23} \left(\frac{V_{SN}}{300\, km/s} \right) \left(\frac{n_e}{10^{-10}\, cm^{-3}} \right)^{-1} cm$$

Ionization length scale of hydrogen due to collision with electrons

Length scale for photo-ionization due to non-thermal UV radiation from the nebula:

$$\lambda_{ph-ion} = \frac{V_{NS}}{n_{ph}\, \bar{\sigma}_{ph}\, c} \approx 3 \cdot 10^{14} \left(\frac{R}{d_S} \right) \left(\frac{\eta_X}{10^{-4}} \right)^{-1} \left(\frac{V_{NS}}{300\, km/s} \right)^{-1} \left(\frac{n_0}{1\, cm^{-3}} \right)^{-1} F(\Gamma)\;\; cm \;\approx\; 10^{14} - 10^{17}\, cm$$

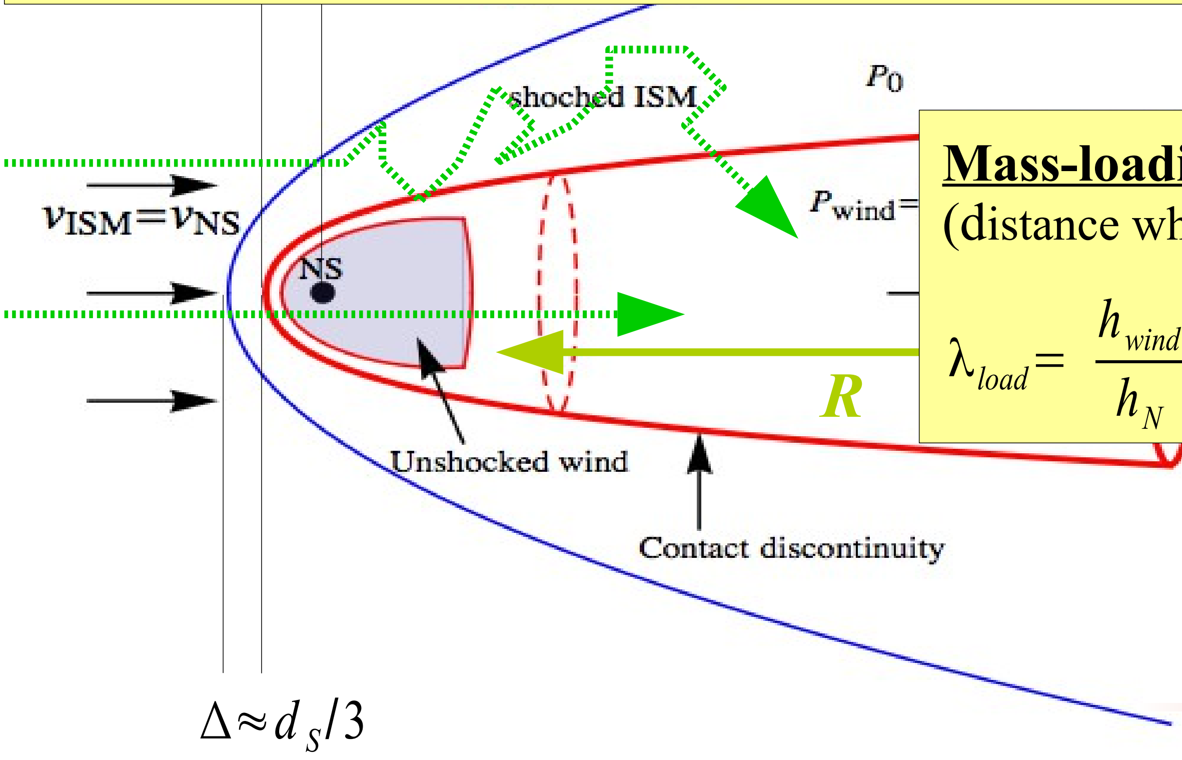

Mass-loading length scale

(distance where mass loaded enthalpy = wind enthalpy):

$$\lambda_{load} = \frac{h_{wind}}{h_N} \frac{V_{wind}}{n_{ph}\, \bar{\sigma}_{ph}\, c} \approx 10^{13} - 10^{17}\, cm \quad \propto \frac{1}{n_{ph}\, n_N}$$

Our quasi 1-D mathematical approach

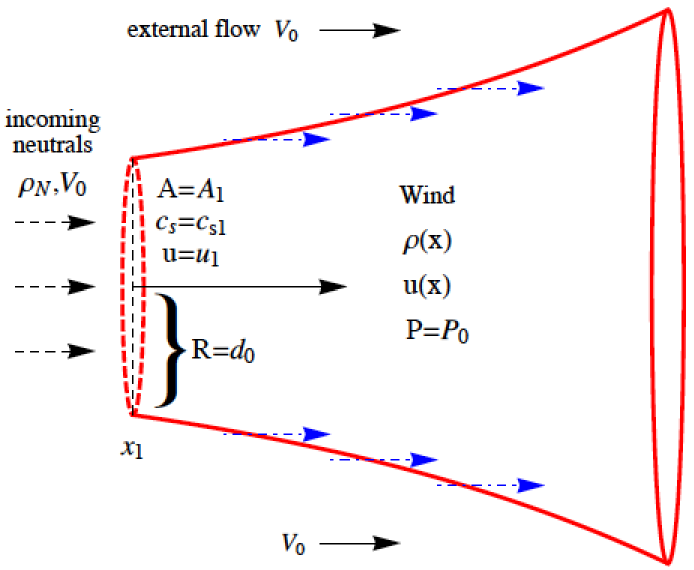

MODEL ASSUMPTIONS

- Stationarity → $\partial_t[\ldots] = 0$
- relativistic e^+-e^- wind plasma
- Cold proton fluid injected through ionization
- Quasi 1-D along the propagation direction x → $A=A(x)$
- No magnetic field
- Ram pressure is neglected

Our quasi 1-D mathematical approach

MODEL ASSUMPTIONS

- Stationarity $\rightarrow$ $\partial_t[\ldots] = 0$
- relativistic e^+-e^- wind plasma
- Cold proton fluid injected through ionization
- Quasi 1-D along the propagation direction x → $A=A(x)$
- No magnetic field
- Ram pressure is neglected

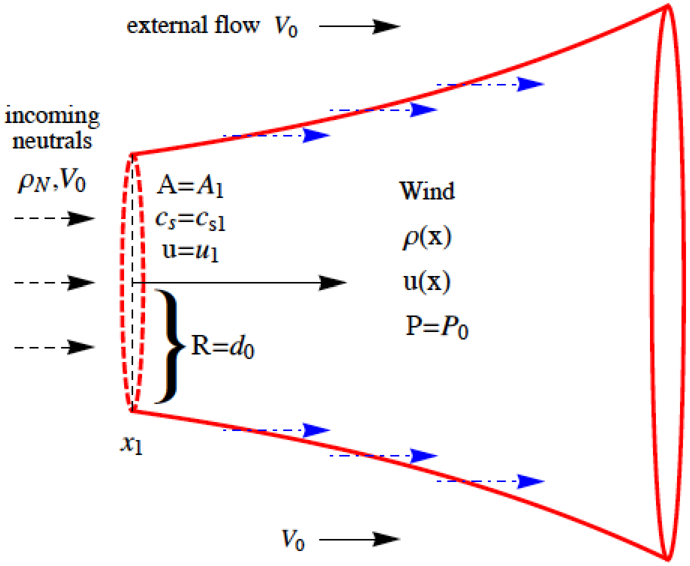

Relativistic conservation equation along the flux tube for a stationary system

$$\partial_x\left[n_{e,p}\, u\, A\right] = \dot{n}_{e,p}\, A'$$

FLUX OF PARTICLE NUMBER

$$\partial_x\left[w\,\gamma_w\, u\, A\right] = q\, c^2 \gamma_0\, A'$$

ENERGY FLUX

$$\partial_x\left[w\, u^2 A\right] + c^2 A\, \partial_x P = q\, c^2 \gamma_o\, A' V_0$$

MOMENTUM FLUX

$$q = \dot{n}\left(m_e + m_p\right)$$
$$\dot{n} = n_N\, n_{ph}\, \bar{\sigma}_{ph}\, c$$

RATE OF MASS LOADING (with constant photon density)

$$P = P_0$$

PRESURE EQUILIBRIUM BETWEEN WIND AND SHOCKED ISM

Our quasi 1-D mathematical approach

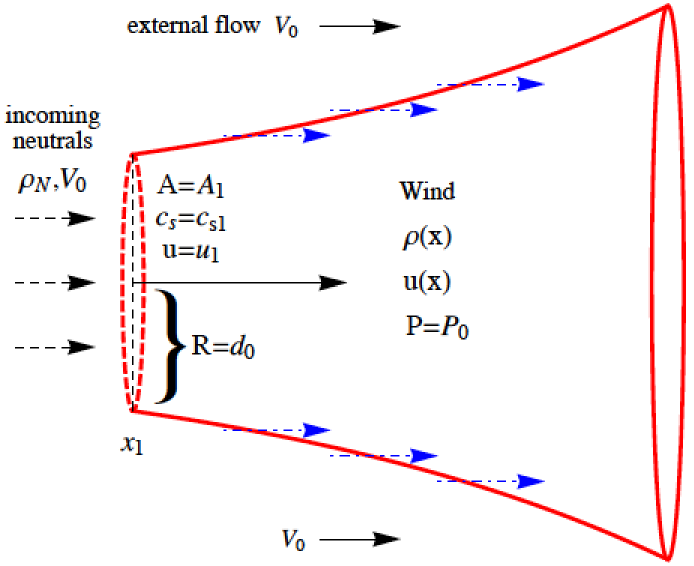

MODEL ASSUMPTIONS

- Stationarity → $\partial_t[\ldots] = 0$
- relativistic e^+-e^- wind plasma
- Cold proton fluid injected through ionization
- Quasi 1-D along the propagation direction x → $A=A(x)$
- No magnetic field
- Ram pressure is neglected

Relativistic conservation equation along the flux tube for a stationary system

$$\partial_x\left[n_{e,p}\, u\, A\right] = \dot{n}_{e,p}\, A'$$

FLUX OF PARTICLE NUMBER

$$\partial_x\left[w\,\gamma_w\, u\, A\right] = q\, c^2 \gamma_0\, A'$$

ENERGY FLUX

$$\partial_x\left[w\, u^2 A\right] + c^2 A\, \partial_x P = q\, c^2 \gamma_o\, A' V_0$$

MOMENTUM FLUX

$$\boxed{A' = A_1}$$

Mass loading only through the initial cross section

$$\boxed{A' = A}$$

Mass loading everywhere

$$q = \dot{n}\left(m_e + m_p\right)$$
$$\dot{n} = n_N\, n_{ph}\, \bar{\sigma}_{ph}\, c$$

RATE OF MASS LOADING (with constant photon density)

$$P = P_0$$

PRESURE EQUILIBRIUM BETWEEN WIND AND SHOCKED ISM

Analytic solution

Analytic solution for relativistic e^+-e^- wind (mass loading everywhere):

$$A(x) = A_1 \frac{u_1}{u}$$

AREA

$$\rho_p(x) = \frac{4P_0}{c} \frac{u_1 - u}{u - V_0}$$

***p* DENSITY**

$$\rho_e(x) = \rho_{e0} + \frac{m_e}{m_p} \frac{4P_0}{c} \frac{u_1 - u}{u - V_0}$$

***e* DENSITY**

$$\frac{x}{\lambda_{load}} = \frac{u}{u - V_0} - \frac{u_1}{u_1 - V_0} + \log\left[\frac{u_1 - V_0}{u - V_0}\right]$$

WIND SPEED

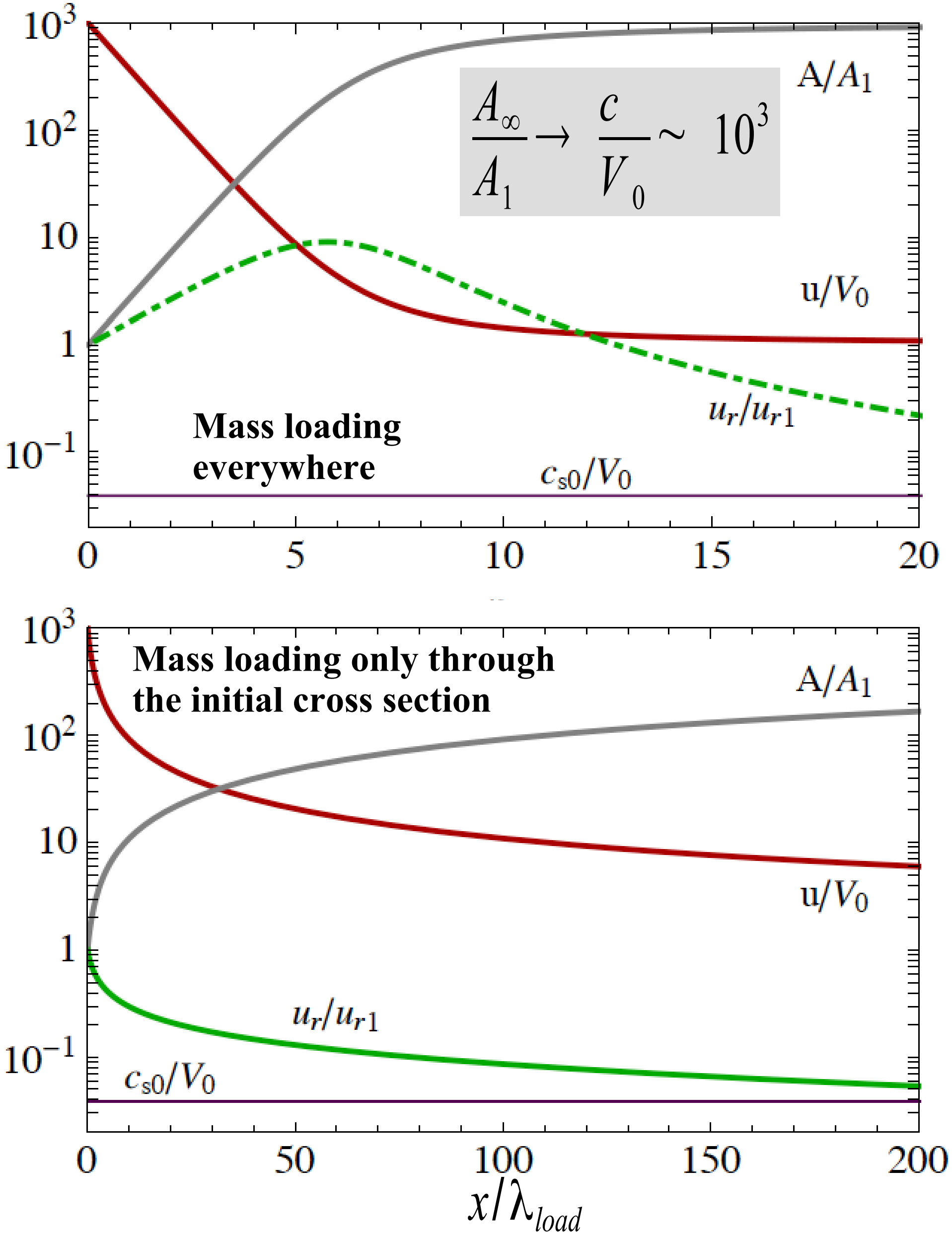

Analytic solution

Analytic solution for relativistic e^+-e^- wind (mass loading everywhere):

$$A(x) = A_1 \frac{u_1}{u}$$

AREA

$$\rho_p(x) = \frac{4P_0}{c} \frac{u_1 - u}{u - V_0}$$

***p* DENSITY**

$$\rho_e(x) = \rho_{e0} + \frac{m_e}{m_p} \frac{4P_0}{c} \frac{u_1 - u}{u - V_0}$$

***e* DENSITY**

$$\frac{x}{\lambda_{load}} = \frac{u}{u - V_0} - \frac{u_1}{u_1 - V_0} + \log\left[\frac{u_1 - V_0}{u - V_0}\right]$$

WIND SPEED

$$u_r(x) = V_0 \frac{d_S}{\lambda_{load}} \frac{u_1^{1/2}(u - V_0)^2}{u^{5/2}} \left(\frac{u}{u_1}\right)^{\frac{1}{2} \pm \frac{1}{2}}$$

RADIAL EXPANTION SPEED

Expansion velocity can be > wind speed

> ISM sound speed

→ stationary quasi 1-D approach no more valid

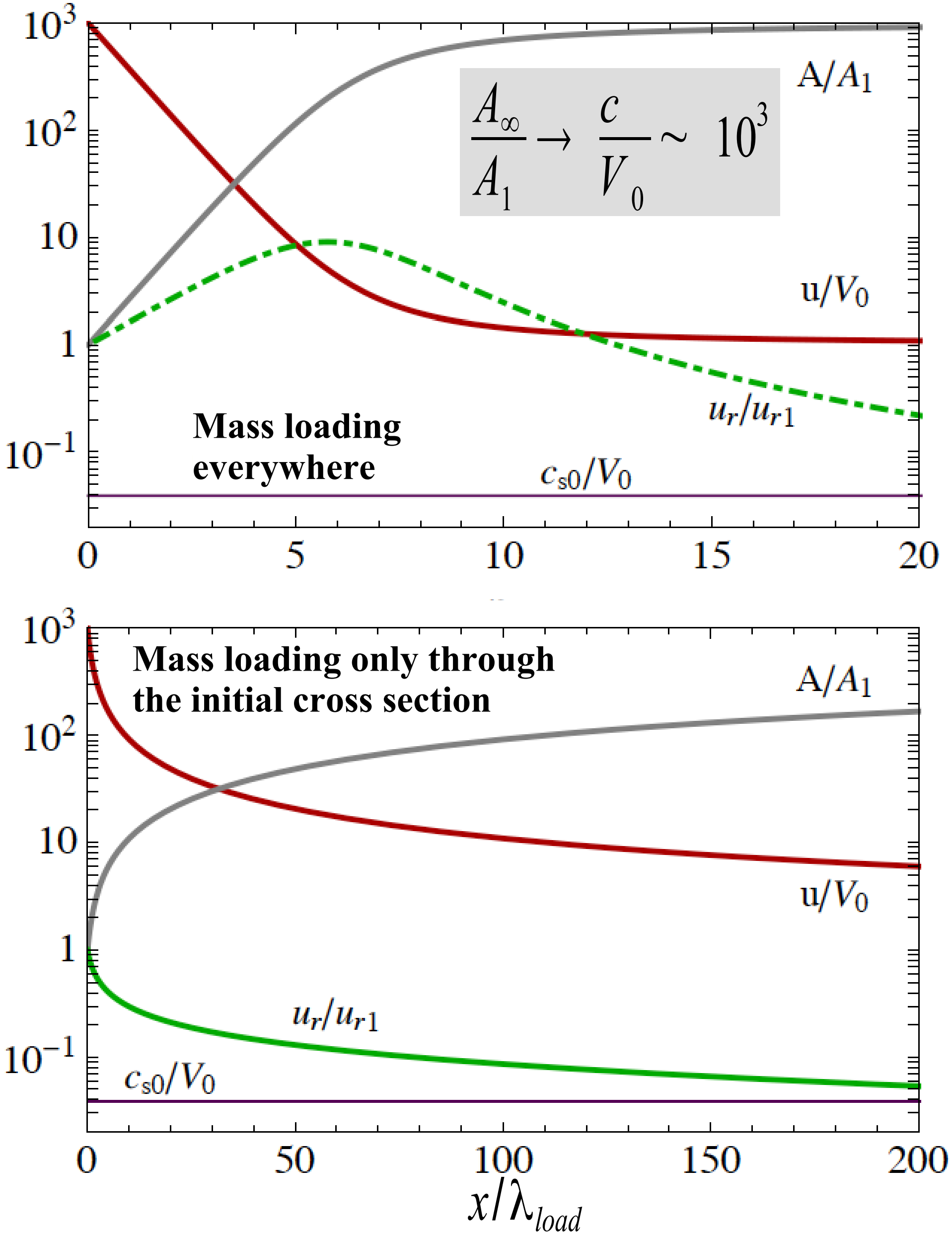

Analytic solution

Analytic solution for relativistic e^+-e^- wind (mass loading everywhere):

$$A(x) = A_1 \frac{u_1}{u}$$

AREA

$$\rho_p(x) = \frac{4P_0}{c} \frac{u_1 - u}{u - V_0}$$

***p* DENSITY**

$$\rho_e(x) = \rho_{e0} + \frac{m_e}{m_p} \frac{4P_0}{c} \frac{u_1 - u}{u - V_0}$$

***e* DENSITY**

$$\frac{x}{\lambda_{load}} = \frac{u}{u - V_0} - \frac{u_1}{u_1 - V_0} + \log\left[\frac{u_1 - V_0}{u - V_0}\right]$$

WIND SPEED

$$u_r(x) = V_0 \frac{d_S}{\lambda_{load}} \frac{u_1^{1/2}(u - V_0)^2}{u^{5/2}} \left(\frac{u}{u_1}\right)^{\frac{1}{2} \pm \frac{1}{2}}$$

RADIAL EXPANTIO SPEED

Scenario A → only through the initial cross section

Scenario B → Mass loading everywhere

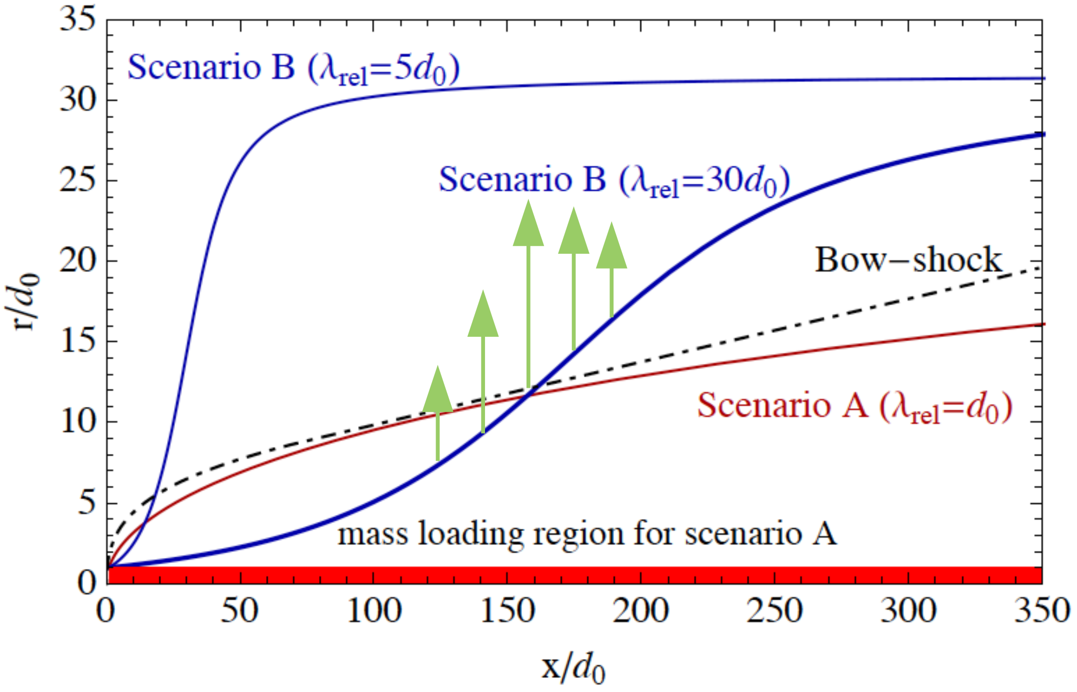

Expansion velocity can be > wind speed

> ISM sound speed

→ stationary quasi 1-D approach no more valid

Analytic solution

Analytic solution for relativistic e^+-e^- wind

(mas

$A($

$\rho_p($

$\rho_e($

$\frac{x}{\lambda_{loc}}$

$u_r($

Exp

→ stationary quasi 1-D approach no more valid

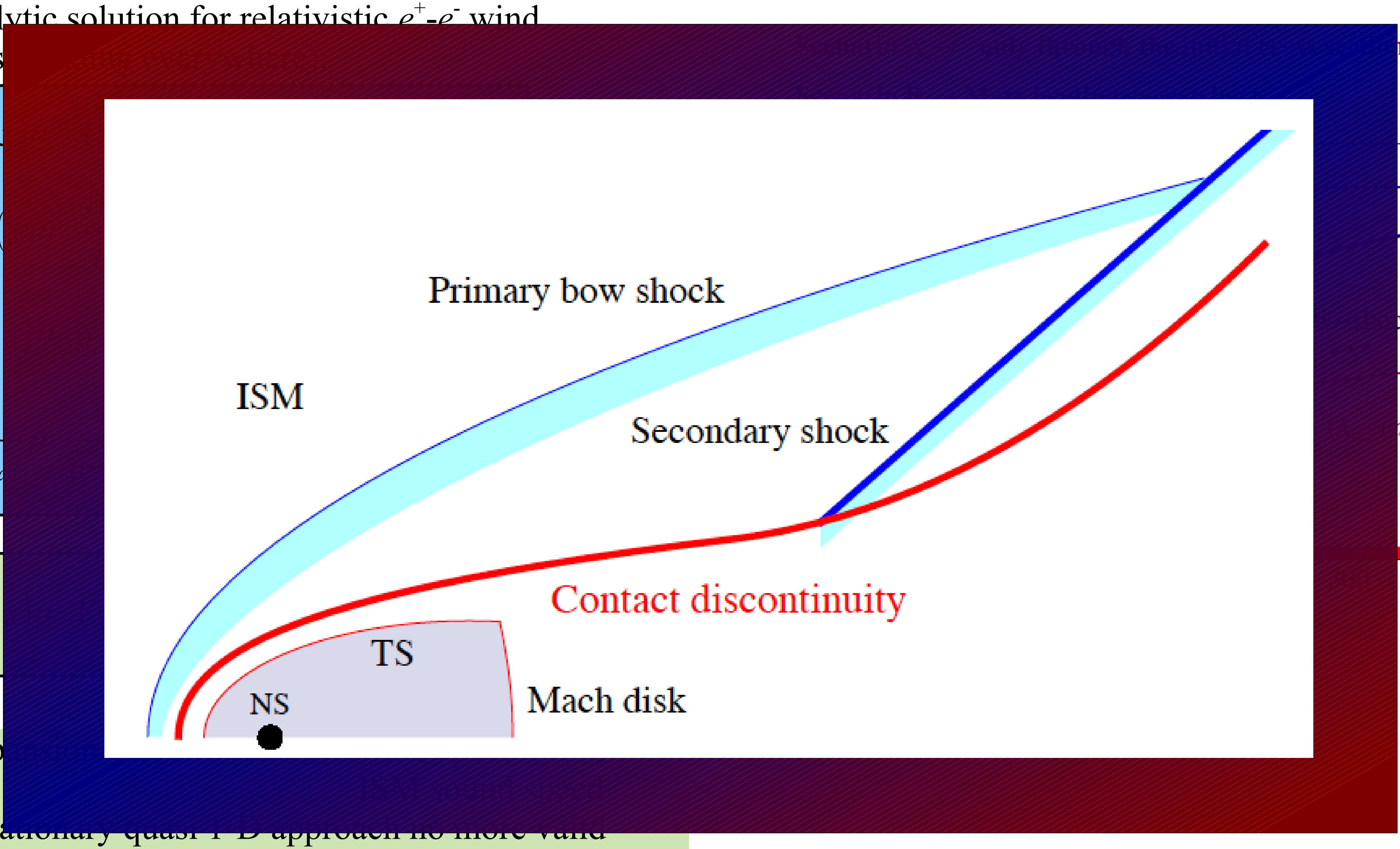

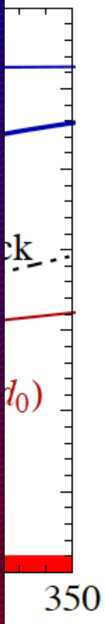

Application to J0742-2822

[Brownsberger & Romani 2014]

$L_w = 1.9\,10^{35}\,erg/s$

$d = 2\,kpc$

$n_{ISM} = 0.28\,cm^{-3}$

$V_\perp = 275\,km/s$

$f_{ion} = 0.5; \quad V_{NS} \approx V_\perp$

$\rightarrow \; d_S$

[FermiLAT data]

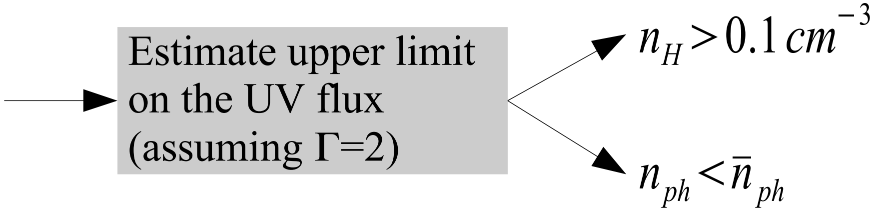

$L_X < 7.6 \cdot 10^{29} \left(\frac{d}{2\,kpc} \right) \frac{erg}{s}$ → Estimate upper limit on the UV flux (assuming Γ=2)

$n_H > 0.1\,cm^{-3}$

$n_{ph} < \bar{n}_{ph}$

$$\rightarrow \lambda_{load} \propto \frac{1}{n_H\, n_{ph}} \approx d_S$$

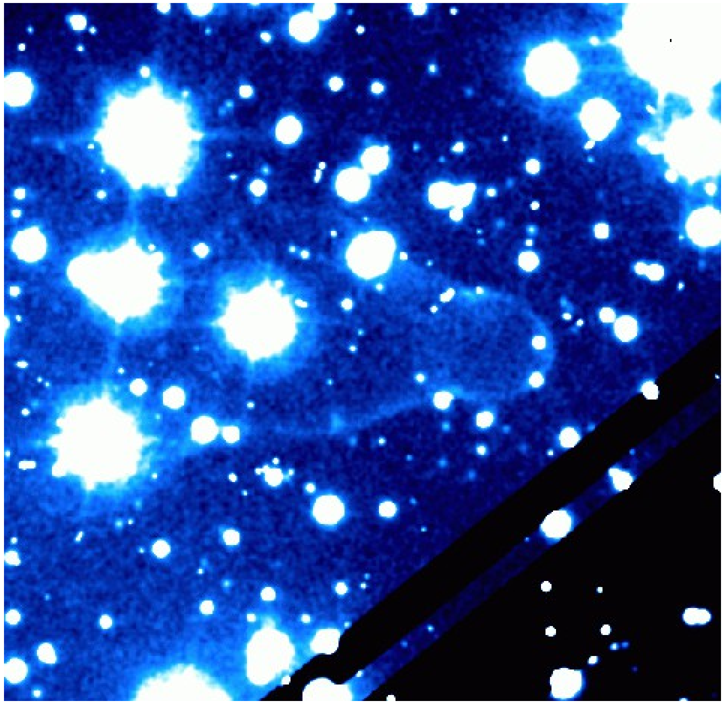

Application to J0742-2822

[Brownsberger & Romani 2014]

$L_w = 1.9\,10^{35}\, erg/s$

$d = 2\, kpc$

$n_{ISM} = 0.28\, cm^{-3}$

$V_\perp = 275\, km/s$

$f_{ion} = 0.5; \quad V_{NS} \approx V_\perp$

$\rightarrow \; d_S$

[FermiLAT data]

$$L_X < 7.6\cdot 10^{29}\left(\frac{d}{2\,kpc}\right)\frac{erg}{s} \longrightarrow$$

Estimate upper limit on the UV flux (assuming Γ=2)

$n_H > 0.1\, cm^{-3}$

$n_{ph} < \bar{n}_{ph}$

$$\rightarrow \lambda_{load} \propto \frac{1}{n_H\, n_{ph}} \approx d_S$$

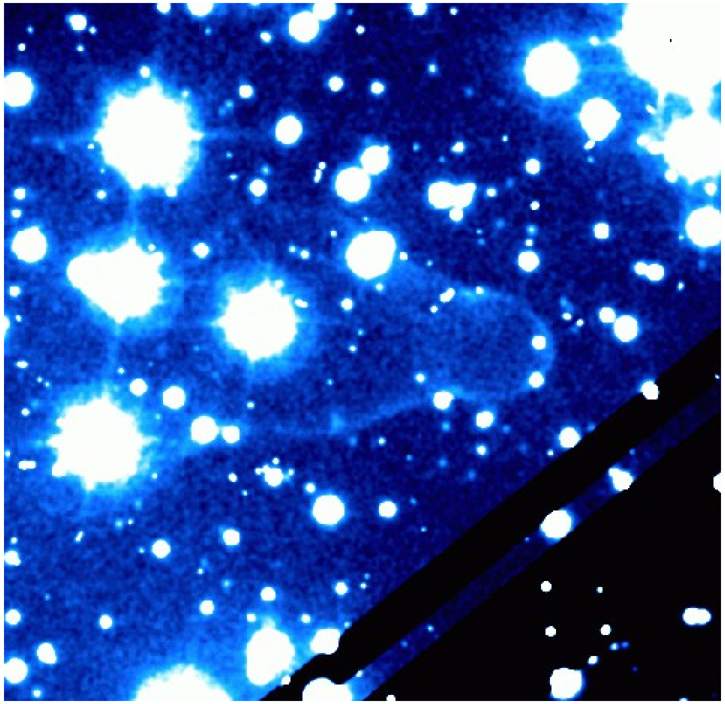

$\lambda_{load} = 2d_S$

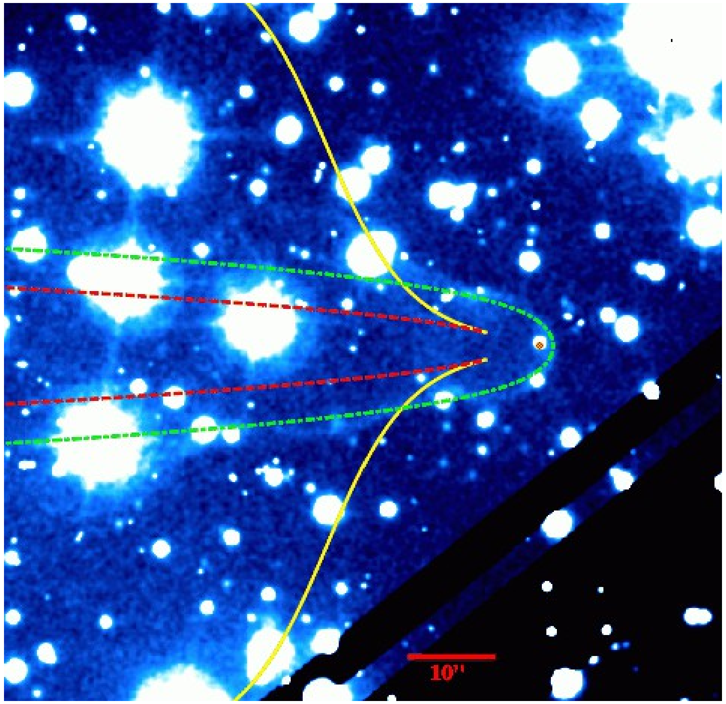

Effect of magnetic field in the wind

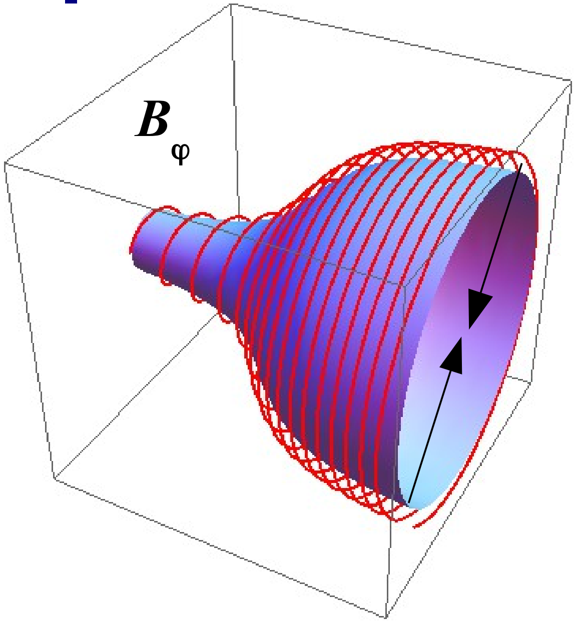

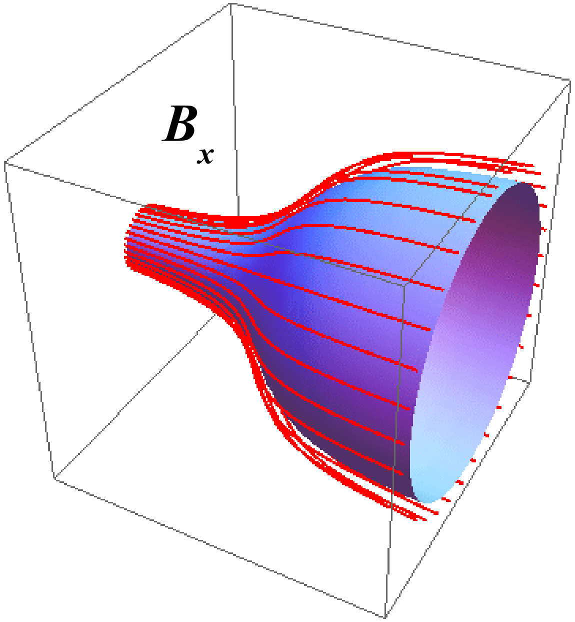

Toroidal component

Magnetic flux conservation:

$$\begin{aligned} &\bar{B}_\phi u_x R = const \\ &R \propto \sqrt{A} \propto u^{-1/2} \end{aligned} \quad \rightarrow \quad \bar{B}_\phi(x) \propto 1/\sqrt{u} \quad \nearrow$$

Poloidal component increases:

→ magnetic hoop stress increases
→ the transverse expansion is reduced
→ **synchrotron emission increases**

$$j_{syn} \propto n_e \bar{B}^2$$

$$n_e u_x A = const \rightarrow n_e = const$$

Poloidal component

Magnetic flux conservation:

$$\bar{B}_x A = const \rightarrow \bar{B}_x(x) \propto u \quad \searrow$$

Poloidal component decreases:

→ No effects on the tale expansion
→ **synchrotron emission decreases**

Mouse PWN vs. PSR J1509-5850

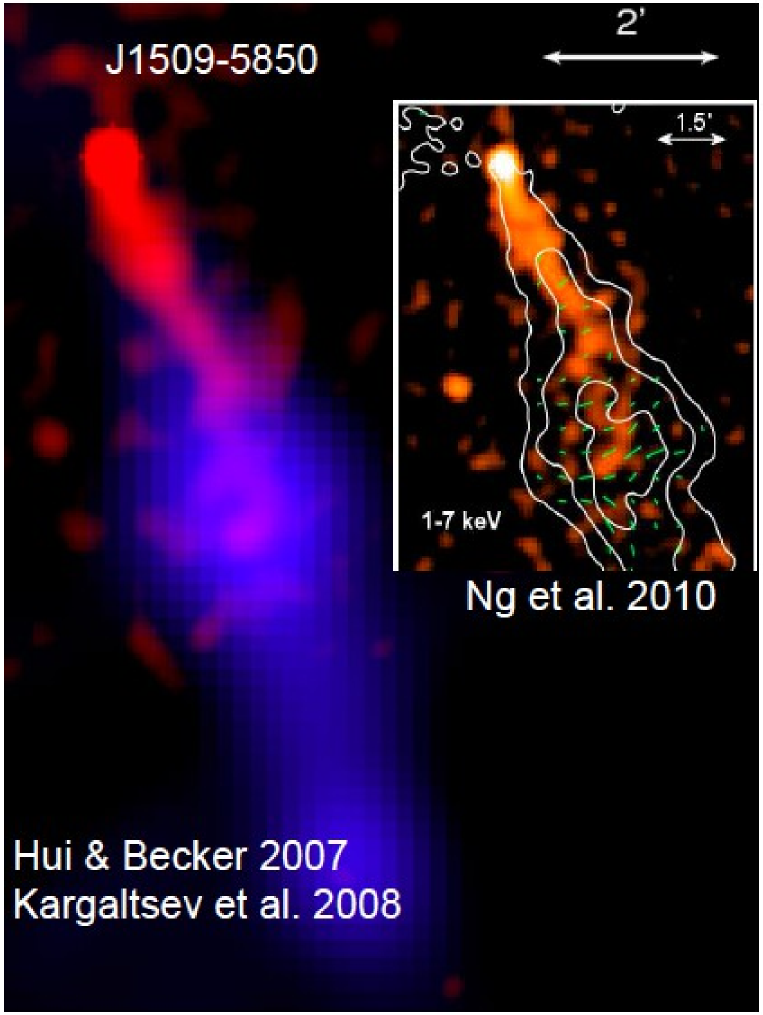

Ng et al. 2010

Hui & Becker 2007
Kargaltsev et al. 2008

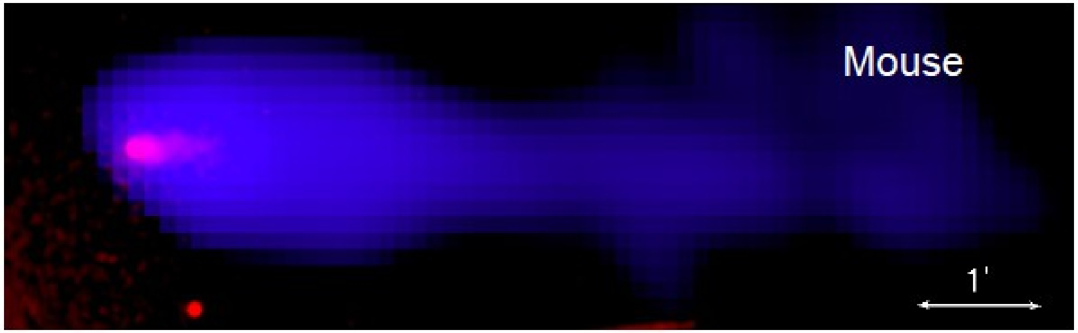

J1509 and Mouse PWNe are different:

- X-ray radio correlation in Mouse vs. anticorrelation in J1509 PWN
  - Anticorrelation is difficult to explain by synch. cooling only
  - In Mouse magnetic field is parallel to the tail, in J1509 tail it is perpendicular.

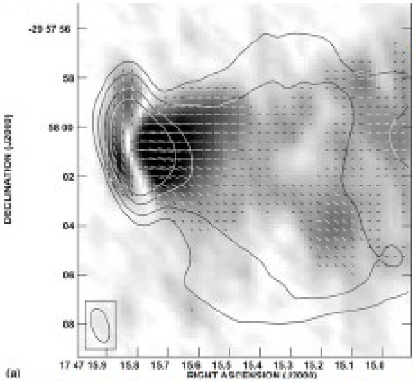

Yusef-Zadeh & Gaensler 2005

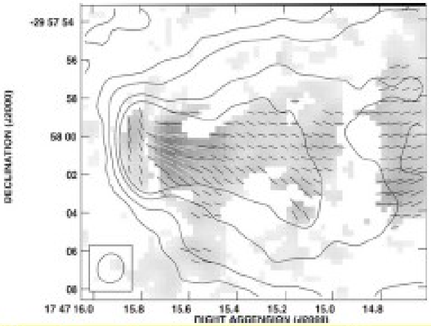

Radio polarimetry provides a unique opportunity to map the magnetic field structure.

Romanova et al. 2005

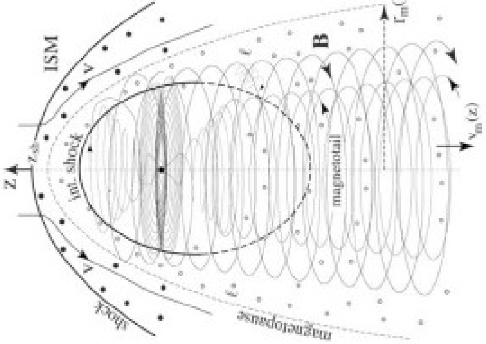

Mouse PWN vs. PSR J1509-5850

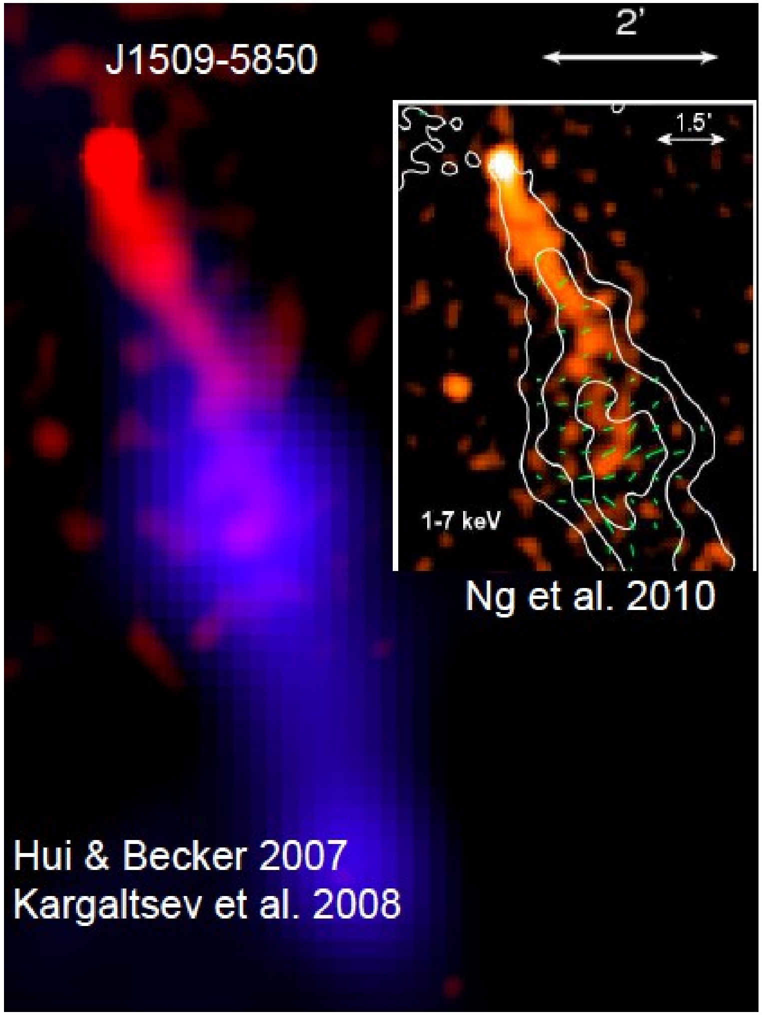

Ng et al. 2010

Hui & Becker 2007
Kargaltsev et al. 2008

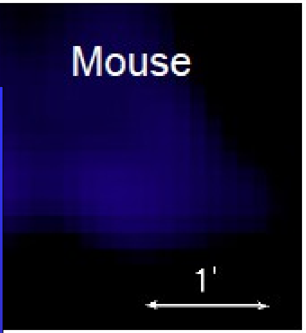

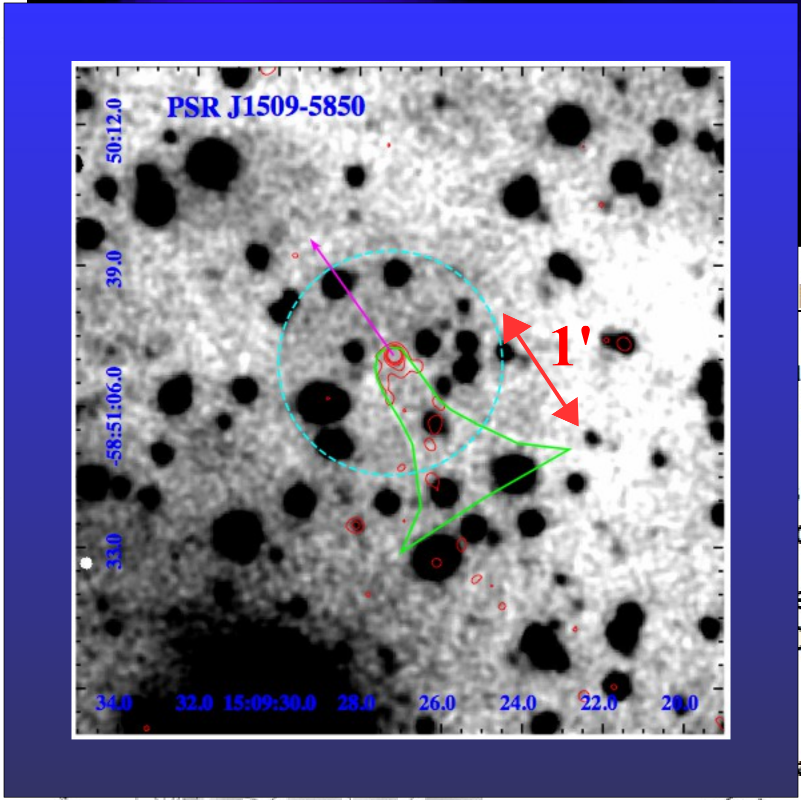

Ne are different:

tion in Mouse
J1509 PWN

difficult to
cooling only

etic field is parallel
09 tail it is

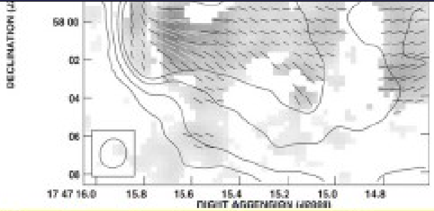

Radio polarimetry provides a unique opportunity to map the magnetic field structure.

a et al. 2005

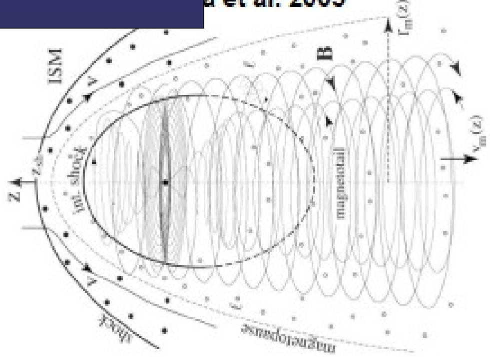

CONCLUSIONS

- **Neutral Hydrogen from ISM can easily penetrate into the relativistic wind of bow-shock pulsar wind nebulae**

- **Internal dynamics of the wind can be strongly affected by neutrals on the typical mass loading scale**
  → ***The flow slows down and expands***
  → ***The expansion can produce secondary shocks where the $H\alpha$ emission is enhanced***
  → ***Secondary shocks can induce the head-shoulder shape observed in many $H\alpha$ nebulae***

- **The stationary quasi 1-D approach fails for very rapid mass loading**
  → ***2D and time dependent simulations are needed to get a comprehensive solution***

- **Magnetic filed cannot be neglected!**